

BUILDING A TURBIDOSTAT TO ANALYZE GUT MICROBIOTA SUCCESSION
IN INFANTS

MSc Thesis - Lucas Flett
McMaster University - Computational Sciences and Engineering

BUILDING A TURBIDOSTAT TO ANALYZE GUT MICROBIOTA SUCCESSION
IN INFANTS

BY

LUCAS FLETT, B.Sc.

A Thesis Submitted to the School of Graduate Studies in Partial Fulfillment of the
Requirements for the Degree Master of Science

McMaster University © Copyright Lucas Flett, 23 November 2018

MSc Thesis - Lucas Flett
McMaster University - Computational Sciences and Engineering

McMaster University Master of Science (2018) Hamilton, Ontario (Computational
Sciences and Engineering)

TITLE: Building a turbidostat to analyze gut microbiota succession
in infants

Author: Lucas Flett, B.Sc.

Supervisor: Dr. Jennifer Stearns

Number of Pages: 84

Abstract

By continually supplying nutrients, a turbidostat presents a steady environment to analyze bacterial growth dynamics. This makes it possible to model microbial community succession in a simple and more realistic way than is possible with batch culture. The problem with current commercial turbidostats are their industrial size and price.

With the use of 3D printed parts, printed circuit boards and laser cut pieces, all readily obtained online and in collaboration with laboratories here at McMaster University, I've created a relatively cheap custom turbidostat, ideally suited for longitudinal studies of microbial consortia that can accommodate eight separate experiments simultaneously. I have modified the design to enable microbial growth at 37°C under anoxic conditions, by changing how the growth media and gas is handled. I have also improved sample collection to make it more convenient and flexible. Cell growth dynamics were interrogated separately with one strain of a facultative anaerobe (*E. coli*) and one strain of an obligate anaerobe (*Bacteroides thetaiotaomicron*) bacteria.

For the individual strains, real-time optical density and dilution rate vs time graphs were created showing that these microbes can be reproducibly cultured, holding steady optical density rates for extended periods of time. Future directions include culturing a complex community without contamination by inoculating the system with microorganisms from an infant stool sample. Community composition and metabolite dynamics could then be analyzed by sampling over time.

Acknowledgments

I would like to thank my supervisor, Dr. Jennifer Stearns. Her patience, and ability to clarify complex microbiology has helped me complete this interdisciplinary thesis. Thank you to my other committee members Dr. Michael Surette and Dr. Zeinab Hosseini-Doust for their expertise, time and support.

Thank you to our lab research assistant Sara Dizzell, she is the first one into the lab and the last one out, always willing to help with a positive attitude. Thanks to Aman Patel, I would have been lost without you. I wish I could have you by my side for all life's future endeavours.

Most importantly thanks to my wife Joti Flett, for being the breadwinner and taking care of her three kids (that is, the twins and I).

Table of Contents

Abstract	iv
Acknowledgments	v
List of Figures and Tables	viii
Abbreviations.....	x
Declaration of Academic Achievement.....	xii
1.0 INTRODUCTION	1
1.1 Microbial Communities	1
1.2 Current Experimental and Culturing Techniques.....	2
1.3 Human Infant Gut Microbiome	7
1.4 Rationale.....	9
1.5 Aims	13
2.0 MATERIALS AND METHODS.....	14
2.1 Building A Turbidostat	14
2.1.1 Printed Circuit Boards	15
2.1.2 Power supply assembly	16
2.1.3 Syringe pump.....	17
2.1.4 Pinch valves	19
2.1.5 Chambers	21
2.1.6 Stoppers.....	24
2.1.7 Software installation.....	25
2.2 Final Assembly.....	26
2.3 Verification of Function.....	27
2.4 Modifications to Improve Reproducibility.....	28
2.5 Modifications to Increase Breadth of Experimental Design	30
2.5.1 Creating custom stir rates in the chambers.....	31
2.5.2 Improving footprint and data acquisition.....	32
2.5.3 Adding compatibility to 37°C environments.....	33
2.5.4 Adding compatibility to dry environments.....	33
2.5.5 Adding compatibility to anaerobic environments	34
2.5.6 Verification of function.....	37
2.6 Culturing A Complex Community	38
2.6.1 DNA extraction and amplification for Illumina sequencing	39
2.6.2 DNA extraction and amplification of contaminants for Sanger sequencing.....	40
2.6.3 Data analysis	42

MSc Thesis - Lucas Flett
McMaster University - Computational Sciences and Engineering

3.0 RESULTS.....	42
3.1 Validation of the original design	43
3.2 Modifications to Improve Reproducibility	47
3.2.1 Pinch valve redesign	48
3.2.2 Altering inoculation technique	48
3.3 Modifications to Increase Breadth of Experimental Design	50
3.3.1 Custom stir bar RPM.....	50
3.3.2 Adding compatibility to dry environments.....	51
3.3.3 Adding compatibility to anaerobic environments	52
3.4 Inoculating a Stool Community.....	54
4.0 DISCUSSION	61
4.1 How Commercial and Other Custom Devices Compare	62
4.2 Contamination Issues.....	64
4.3 Future Directions	66
4.3.1 Reproducibility	66
4.3.2 Contamination.....	67
4.3.3 Future experiments	67
5.0 LIMITATIONS	68
5.1 Limitations of This Turbidostats Design.....	68
6.0 CONCLUSION.....	70
7.0 REFERENCES	71
8.0 APPENDIX I	82
8.1 Protocols	82
8.1.1 Remotely visualizing the Pi	82
8.1.2 Remotely transferring data from the Pi.....	83
9.0 SUPPLEMENTARY MATERIALS.....	84

List of Figures and Tables

Figure 2.1.1: Schematic of turbidostat.....	14
Figure 2.1.1.1: Chamber PCB.....	16
Figure 2.1.2.1: External power supply.....	17
Figure 2.1.3.1: Syringe pump.....	19
Figure 2.1.4.1: Pinch valves.....	21
Figure 2.1.2.1: Stir motors and chambers.....	22
Figure 2.1.5.1: Glass coverslip.....	23
Figure 2.1.6.1: Stopper mold and final product.....	25
Figure 2.2.1: Final assembly.....	27
Figure 2.4.1: Pinch valve redesign.....	29
Figure 2.5.4.1: Humidifier.....	34
Figure 2.5.5.1: Stopper redesign.....	36
Figure 3.1.1: Optical density of <i>E. coli</i> BL21 over time.....	44
Figure 3.1.2: Dilution rate of LB over time.....	45
Figure 3.1.3: Commercial plate reader vs turbidostat.....	46
Figure 3.2.1.1: Different inoculate volumes.....	47
Figure 3.3.1.1: Voltage vs RPM.....	49
Figure 3.3.3.1: <i>Bacteroides</i> OD ₆₅₀ vs time.....	51
Figure 3.3.3.2: Sample plated from the turbidostat.....	52
Figure 3.4.1: Stool community plated before and after turbidostat.....	54
Figure 3.4.2: ASV relative abundances at each sample point	55

Figure 3.4.3: Shannon diversity index over time.....	56
Figure 3.4.5: Measuring the reproducibility of diversity.....	57
Figure 3.4.6: The five most abundant bacterial phylotypes (ASVs) over time....	58

Abbreviations

ABS	Acrylonitrile butadiene styrene
ASV	Amplicon sequence variant
BHI	Brain heart infusion broth
CAD	Computer aided design
CNA	Columbia agar
CNC	Computer numerical control
HMO	Human milk oligosaccharide
I_{MAX}	Maximum current
LB	Lysogeny broth
MAC	MacConkey agar
OD	Optical density
OD₆₅₀	Optical density measured using a 650 nm light source
PCB	Printed circuit board
Pi	Raspberry Pi Zero
R_{cs}	Current sense resistance
RPM	Revolutions per minute
SCFA	Short chain fatty acid
SCIMP	Starch, carboxymethyl cellulose, inulin, mucin, pectin
SDS	Sodium dodecyl sulfate
TSA+B	Tryptic soy agar with 5% sheep blood
V_{REF}	Reference voltage

WLB Worm lysis buffer

Declaration of Academic Achievement

The majority of engineering, experiments, data acquisition and analysis was performed by Lucas Flett. Supervisor Dr. Jennifer Stearns was a significant contributor to experimental designs, committee members Dr. Michael Surette and Dr. Zeinab Hosseini-Doust provided guidance. 16S rRNA gene sequencing was performed by McMaster Metagenomics Facility.

1.0 INTRODUCTION

1.1 Microbial Communities

Microbial communities are groups of microorganisms, consisting of multi-species assemblages which interact with one another and live together in a contiguous environment ¹. The interactions, population dynamics and functionality of these communities have a significant impact on both the environment and human health ^{2,3}. These microorganisms (or microbes) include all unicellular organisms such as bacteria and protists, as well as some larger multicellular organisms like fungi; recent estimates have microbes comprising over half of the world's biomass ⁴. Microbial communities are all around us, and a part of every ecosystem on the planet. They play crucial roles that we cannot live without. For example, environmental microbial communities are responsible for the cycling of carbon, nitrogen, phosphorus and sulfur on the planet ⁵. Additionally, microbial communities are essential for human health as they are involved in nutrient breakdown, metabolic regulation, immunological processes, and physiological functions ^{6,7}.

To better understand the interplay of these groups of microorganisms, we study the interactions they encounter with each other and their environment. This field is known as microbial ecology. Due to the large number of interactions between microorganisms in a community, studying a community's structure and function is challenging ^{8,9}. The microbial ecology within the human gastrointestinal tract (gut) is an example of one such complex system. The microbiota of the gut

have many important functions in digestion, vitamin production and resistance to colonization by pathogens ². However, our understanding of the complex ecological networks formed within the gut between bacteria, viruses and fungi is limited ¹⁰. The colonization of the human gut in infancy and the alterations in community structure as the community stabilizes are particularly interesting from the perspective of microbial ecology ¹¹.

By studying these complex communities, investigators aim to examine how communities change over time, how biological clusters are assembled and how they functionally interact ¹. The more recent development of 16S rRNA gene sequencing has highlighted the great amount of species richness and diversity in microbial communities of both environmental and human samples ^{12,13}. Within laboratory environments, it is difficult to replicate the complexity of these bacterial communities ¹⁴. Furthermore, the ability to study these communities longitudinally has proven to be difficult in standing culture, because of the stress imposed by the accumulation of waste products and dwindling nutrients ^{15,16}. Therefore, it is essential for new developments to be made to study these complex communities ^{17,18}.

1.2 Current Experimental and Culturing Techniques

Due to the complexity of microbial communities, ecologists create models to test their hypotheses. To explain the cause of biodiversity in a given environment, factors such as available resources, pairwise interactions between community members and any perturbations made to the system are taken into

consideration ¹⁵. Given these factors, biodiversity is studied by measuring population sizes of community members over time ¹⁹. Theoretical models of these ecosystems need to be simplified as they cannot account for every variable. One of the first ecological models, known as the Lotka-Volterra or predator-prey model, estimates how the number of individuals in each population (predator and prey) changes over time with two simple differential equations. The prey's rate of population change is proportional to its initial population minus the rate at which it is preyed upon. The predator's population change is proportional to its rate of consuming prey minus its death rate ²⁰.

There have been some useful applications of this model in microbial ecology, such as being able to predict population dynamics of bacteria and bacteriophages ²¹. The problem with this model is its simplicity; the rules of the world it creates are different from reality. One such rule is the competitive exclusion principle, which states that two species cannot live together in a stable equilibrium if they are both competing for the same limited resource ²¹. Thus, if one species has a slight advantage over the other, it will drive the other one to extinction when given sufficient time. However, this does not happen in nature, as there are many instances of species being able to coexist in the same habitat while competing for the same limited resource ^{22,23}.

Since then, microbial ecology models have come a long way, for example with the ability to incorporate the effects of commensalism. This is realized by adding the effects of spatial heterogeneity to the model, where population dynamics are driven by state spaces constructed by spatial boundaries ^{24,25}.

Biofilms have also been modeled with success in a similar way²⁶. These are based on the cellular automaton model²⁷, where a grid of cells is created based on the physical environment of interest, with each cell representing a state that can influence its neighboring cells.

Even if contemporary models can accurately describe population dynamics, the natural phenomenon of horizontal gene transfer can lead individuals to function very differently from other members of the same species²⁸. Given the gradient of diversity that likely exists, new models should be based on individual cells of the community if they want to accurately describe community dynamics. In this case current computing power could only handle the simplest of synthesized scenarios. Another solution to modeling microbial ecology could take the entire system as one entity, one that could be described by its functions such as metabolites and proteins²⁹.

Once a microbial ecology model has been theorized, empirical data needs to be collected to fine tune the parameter estimations. Comparing these theories to field experiments can be tedious⁸. It is not possible to account for all the variables in a field experiment, they are too complex, and hence reproducibility becomes an issue. The model becomes too general to explain a real community. Theoretical and field studies of microbial ecology can be bridged and reinforced with laboratory experiments¹⁵. In the lab, complete control can be exerted over the system. Parameters can be adjusted and measured. Complexities can be added or taken away. Due to the small size of bacteria, ecological experiments in the lab can be replicated much more easily than field experiments.

Many microbial experiments in the lab are done in broth or on solid media. For example, a certain microbe of interest can be isolated using a selective media³⁰. However, this culturing method has its limitations. Long-term community interactions cannot be accurately studied because the nutrients are finite, generally depleted within several of days. This type of closed system allows the study of variable nutrient dynamics over a brief period. To study entire microbial communities and their interactions over extended periods of time, a different approach that removes the problems of waste accumulation and nutrient limitation is required.

One approach to bypassing waste accumulation and nutrient depletion in the study of microbial communities over time is the use of a continuous culture device. The first microbial continuous culture device was invented in 1950³¹. A chamber was filled with liquid media and inoculated with microorganisms like bacteria or yeast. As the media was consumed and the microbes multiplied, fresh media from a media reservoir was added to keep the microbes growing at a constant rate. Effluent was taken away at the same rate that fresh media was added to keep the chamber volume constant. There have been two main variations of this device, namely a chemostat and an auxostat³². They differ based on the way they add fresh media to the chamber. A chemostat adds media at a fixed rate predetermined by the experimenter. An auxostat adds media at a variable rate based on a threshold (predetermined by the experimenter) related to the biomass concentration in the chamber.

Many types of auxostats exist because there are multiple methods to measure the biomass concentration. A pHauxostat³³ measures the pH of the chamber and only dilutes fresh media if a pH threshold has been reached. As the cells continue to grow in the chamber they will change the pH of the solution, but the new media added contains a buffer that mitigates that change. A stable equilibrium is reached at the threshold pH. This pH (and therefore biomass concentration) is maintained where the cells are able to grow at a constant rate. Another example of an auxostat is a permittostat³⁴, which measures the dielectric permittivity of the chamber's solution. An electric field is applied to the solution that polarizes the cells inside. The greater number of polarized cells in the solution, the greater amount of charge is needed to generate one unit of flux through the solution. A dielectric spectrometer is used to measure this charge (or permittivity) and dilutes media once the permittivity threshold has been met.

A third variant of an auxostat is called a turbidostat³⁵. Diluting media is regulated by the turbidity (or optical density) of the solution. The optical density is constantly updated by measuring the amount of light that transmits through the solution. As a solution becomes more dense, less light is able to transmit through it, and so the optical density increases. If the optical density increases past the threshold set by the experimenter, new media is pumped into the chamber. By setting an initial optical density, a turbidostat can vary its nutrient supply until the desired turbidity has been reached. That density will remain for the entirety of the experiment. In this way, a turbidostat (and all other continuous culture devices) can model community dynamics for as long as the experimenter has new media.

A continuous culturing system would allow long-term laboratory experiments, with microbial ecologists able to study important aspects such as evolution, community succession and bacterial cross-feeding³⁶. Evolution can be studied by sampling from the chamber over a long period of time. Time series analysis can then be performed on microbial genomes³⁷. Succession could be studied by observing the changes to the community's composition as it moves from initial inoculation to a stable community³⁸. Different microbes could be externally added to the system during this process to simulate the natural addition of new members to a community. Bacterial cross feeding involves one bacterium using another bacterium's byproduct as an energy source. The secondary degraders could be externally added once the primary degraders have produced a sufficient amount of byproducts^{39,40}. Another option could connect two continuous culture devices together. The first device would contain the primary degraders with their ideal media source. The second device would use the effluent of the previous device as a media source, which should be full of byproducts for the secondary degraders to metabolize.

1.3 Human Infant Gut Microbiome

The microbes that colonize the human digestive tract, along with their genomes and environmental conditions collectively known as the human gut microbiome⁴¹ has garnered a lot of interest as of late, due its association with metabolic and immune health¹¹. These associations are even more pronounced in infants as their gut microbiome and immune system are developing¹¹. During

infant development the gut microbial community is unstable, and any perturbations to the system, including antibiotics, formula feeding and weaning could have long lasting effects before the community becomes adult-like between one and three years of age ¹¹. In particular, breastfeeding is one of the key factors that determines the microbial composition of the infant gut ⁴². Human milk oligosaccharides (HMOs) are indigestible sugars only found in breast milk, and only species from two bacterial genera are known to metabolize these in the gut, *Bifidobacterium* and *Bacteroides*. Infants who are breastfed have higher relative abundances of these species compared to formula fed infants ⁴³. The byproducts of *Bifidobacterium* and *Bacteroides* metabolizing HMOs include short chain fatty acids (SCFAs), which plays a crucial role in the development of the immune system ⁴⁴.

Bifidobacterium and *Bacteroides* are sensitive to oxygen and must be cultured under anaerobic conditions. Studying these microbes individually in a continuous culture device could lead to understanding their preferred growth conditions and interactions with other bacteria.

Current methods to study the infant gut usually involve sampling infant stool and measuring its bacterial composition by 16S rRNA gene sequencing ¹¹. This provides a rough idea of the taxonomic diversity in the gut. The problem with this method is the lack of information it provides about the community's function, and that it only shows bacterial diversity. Other members of the community such as fungi, viruses and archaea are not accounted for. Shotgun metagenomic sequencing involves sequencing all of the microbial genes in the community, but

this method is expensive and lacks the sensitivity of marker gene (e.g., 16S) or culture dependent methods ⁴⁵.

To get a more robust understanding of the ecology in the infant gut microbiome it is important to consider both holistic and reductionist approaches ⁴⁶. While arguments have been made for evaluating the community as a whole ^{47,48}, reducing the system to individual strains of bacteria can illuminate simpler, foundational properties of the community that affect community dynamics. The concept of keystone species was introduced from macroecology in 1969 and describes how one species (e.g. predator) can be responsible for the diversity of a community, which is demonstrated by removing the species and observing lower community diversity ⁴⁹. This concept has since been hypothesized to occur in the gut microbiome, where certain species of bacteria would be responsible for disproportionately influencing a community in compositional and functional ways ^{44,50}. For example, providing ideal growth conditions for *Bifidobacterium* and *Bacteroides* might encourage greater SCFA production by other members of the community.

1.4 Rationale

We would like to use a continuous culturing system *in vitro* that enables the study of community dynamics over time. By sampling on demand, we can study aspects of microbial ecology that are impossible with current plating methods. Of all the continuous culture devices to choose from, the turbidostat was chosen based on price and ease of fruition. Commercial continuous culture devices can

cost hundreds of thousands of dollars, most of which are scaled for mass production ^{51,52}. A small inexpensive commercial device suited for laboratory experiments does not exist. Because of this gap some microbiology engineers have developed open source custom continuous culture devices ^{53,54}. With most research facilities having access to Computer Numerical Control (CNC) machines, 3D printers, and the ability to purchase any other needed hardware online, these devices can be built by someone with no formal engineering background. The majority of these open source devices are chemostats or turbidostats because they are the easiest and most cost-effective to build. In contrast to a permittistat which needs a dielectric spectrometer, a turbidostat can measure its biomass concentration with an economical laser pointer and a sensor that converts light intensity to frequency. A chemostat is even simpler as it does not require a measurement relating to biomass concentration. Since a chemostat dilutes media at a predetermined rate, all that is needed is a computer controlled media pump. I chose the turbidostat over the chemostat in order to perform experiments that involved stabilizing a community of microbes to discern measurable changes when that community is challenged with controlled perturbations. A turbidostat is favored over a chemostat for long term stability as chemostats are more likely to create evolving communities ⁵³. For a chemostat to function properly, the media used needs to contain a limiting nutrient ⁵³. This is so that an equilibrium can be reached, a steady growth rate where the microbes have maxed out the limiting nutrient at the same rate the media is pumped. Since the community has a limited nutrient, it can evolve to select for microbes that utilize this nutrient in the most efficient way.

In this way a chemostat could be a better choice if evolution or nutrient limiting environments wanted to be studied. Studying community succession and stabilization with unlimited resources is better suited to turbidostats.

The turbidostat chosen to be built was based off of Takahashi et al. 2015 paper ⁵³ because it is cost-effective, has detailed build instructions and has the ability to run eight experiments in parallel. The most complicated parts were built using basic servo motors, printed circuit boards (PCBs) and 3D printed parts, requiring very few expensive commercial parts. A website is dedicated to help fellow microbiologists build this turbidostat. Files are available to download the layout of the PCBs, 3D printed and laser cut parts, along with a full set of instructions and illustrations to construct the turbidostat. ⁵³ suggests that the turbidostat can be built for under \$2,000 USD. An additional strength of the turbidostat is the reproducibility implications. Many of the open source turbidostats were designed with only one or very few chambers to inoculate ⁵⁴. Historically, microbial community experiments done in continuous culture devices have not examined the reproducibility of their findings ⁸. With the ability to run eight separate experiments simultaneously, many areas of study can be checked for reproducibility including community composition, time to stabilization of the community and metabolite production. There are several open source documents describing the turbidostat model ^{54,55}, however, other sources are often far more expensive or lack a sufficient amount of chambers.

Although auxostats do not suffer from the same evolutionary bias chemostats do, they still have their own limitations. Specifically turbidostats need

a light source to shine through the solution to measure its optical density. If the media is inherently opaque, or the biomass concentration becomes dense enough to prevent the light from transmitting, the optical density measurement will not be accurate ³⁴. This means turbidostats cannot be used with certain medias or biomass concentration levels. Other auxostats like the pHauxostat and permitistat do not have this problem. Yet experiments using a pHauxostat are limited to those with microbes that significantly change the pH of a solution, as well as having a media that can properly buffer them ³³. Problems with a permittitstat's permittivity measurement can occur if the physiology of a microbe changes over its lifetime, impacting its ability to be polarized ³⁴. Since mass production was not an objective, and the media used was transparent, the density limitations of turbistoats would not affect the experiments.

The infant gut microbiome is of particular interest to our study of microbial ecology for two main reasons. Firstly, the infant gut diversity is relatively low, leading to simpler analysis of interactions ⁵⁶. Secondly, the system is also much more volatile and still developing compared to an adult microbiome ¹¹. This means community succession should be more prevalent and easier to study. But culturing these microbes is a challenge, because they prefer the environmental conditions of the gut. To assess the tubidostat's ability to function continuously, anaerobically, and at 37°C, initial experiments were conducted using a single strain of bacteria. Type strain *Bacteroides thetaiotaomicron* (ATCC 12290) was strategically chosen as the first bacteria to evaluate the turbidostat's ability to support anaerobic growth as it is a known infant gut colonizer ⁵⁰, and is an obligate anaerobe. Complexity

can then be increased by adding additional members to the community, eventually leading to inoculating a stool sample. With the ability to run eight separate experiments in parallel, many combinations of bacteria can be studied at the same time to help elucidate how these microbes interact.

1.5 Aims

Aim 1: Construct a continuous culture turbidostat device.

Aim 2: Modify the continuous culture turbidostat device to work anoxically at 37°C.

Aim 3: Explore the ability of the continuous culture turbidostat device to support the growth of oxygen sensitive bacteria at 37°C.

2.0 MATERIALS AND METHODS

2.1 Building A Turbidostat

A continuous culture turbidostat device was built according to ⁵³. A brief summary of the steps are outlined below along with all modifications to the design. The turbidostat is composed of two main systems: fluid handling and culture tubes (schematic in Fig. 2.1.1), that are automated and allow automatic dilution rates based on the optical density (OD) of the culture.

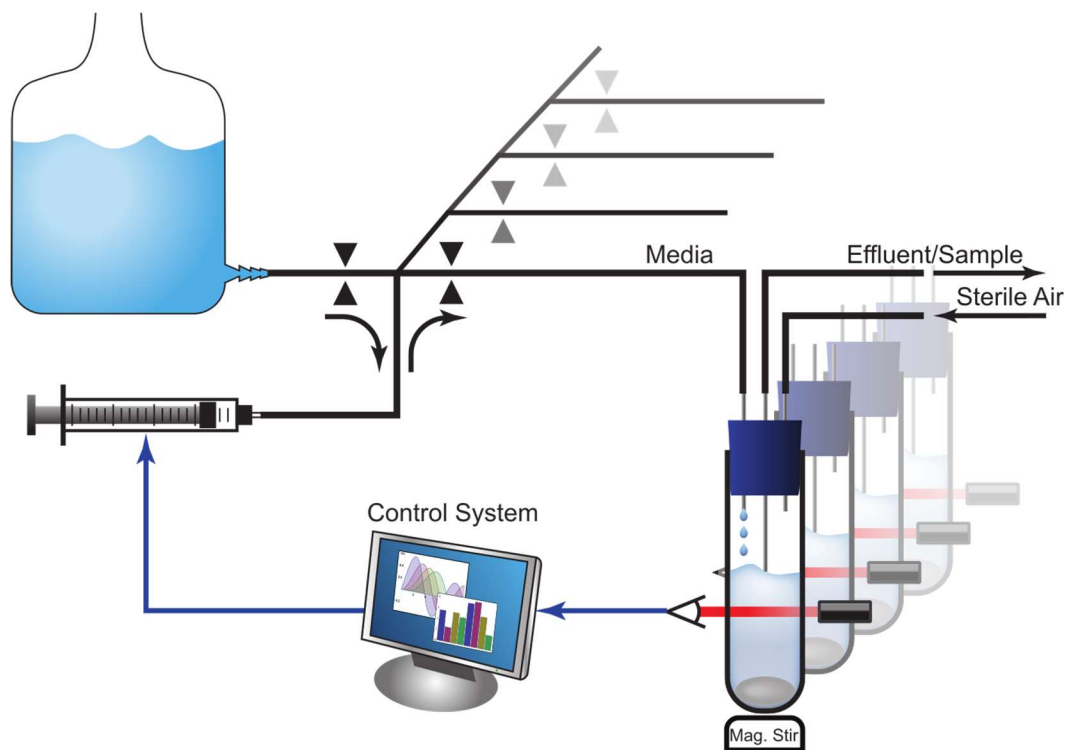


Figure 2.1.1: Schematic of turbidostat ⁵³.

OD is measured cross sectionally through each chamber and relayed to the control system. Comparing the measured OD to a preset threshold OD determines the dilution rate administered by the pump system. The eight chambers running in parallel are cycled through using a pinch valve system.

The fluid flows from a 5 L media bottle with a spout at its base acting as an unlimited media reservoir to the eight culture tubes acting as eight separate experiments. Effluent is taken out of the culture tubes at the same rate fresh media is added to keep each culture tube at a constant volume. The media bottle is placed above the culture tubes allowing the media to flow due to the force of gravity. Two aquarium pumps (Silent-Air X5, 80 Gallons) pull air from their environment and force it into the culture tubes, creating enough positive pressure to pull liquid out of an effluent pipe if the culture tube begins to exceed the original volume.

Each chamber (test tube) has a 650 nm laser that transmits through the solution to a photo detector on the other side. The amount of light that transmits through the solution is sent to the control system and recalculated into an OD_{650} reading. New media is added if the chamber's optical density exceeds the predetermined threshold OD_{650} .

The chamber OD_{650} readings are measured every minute and media flow is regulated to keep each chamber at its threshold OD_{650} for the remainder of the experiment.

2.1.1 Printed Circuit Boards

The control system is a combination of software running on a laptop and custom printed circuit boards (PCBs) ⁵⁷. Eight identical PCBs (Seeed studio) were ordered partially assembled for the eight chambers. Two photodetectors (Sparkfun, TSL235R) were soldered onto each of these PCBs (Fig. 2.1.1.1) to measure the optical density of each chamber. The individual chamber PCBs were

then connected to a central PCB (Seed studio) that joins the chambers to the remaining components of the system. Together, these PCBs regulate the flow of the media based on the optical density readings through their individual microcontrollers.

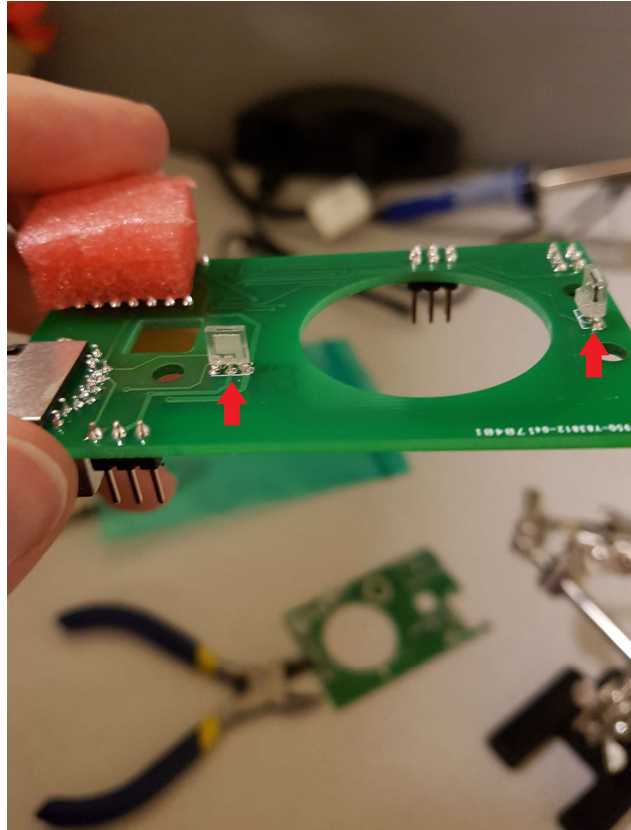


Figure 2.1.1.1: Chamber PCB.

Red arrows show where light sensors are soldered. One sensor (left) is used to improve the signal to noise ratio, while the other (right) records the amount of light transmitted through the chamber.

2.1.2 Power supply assembly

The external power supply (MEAN WELL, 323505) was connected to the central PCB by stripping heavy gauge 4 conductor wire, crimping them to connector pins and inserting those pins into a Molex connector housing (Digikey, WM6982-

ND) (Fig. 2.1.2.1). To connect the power supply to an electrical outlet, a 3-prong power cord was stripped and connected to the external power supply.

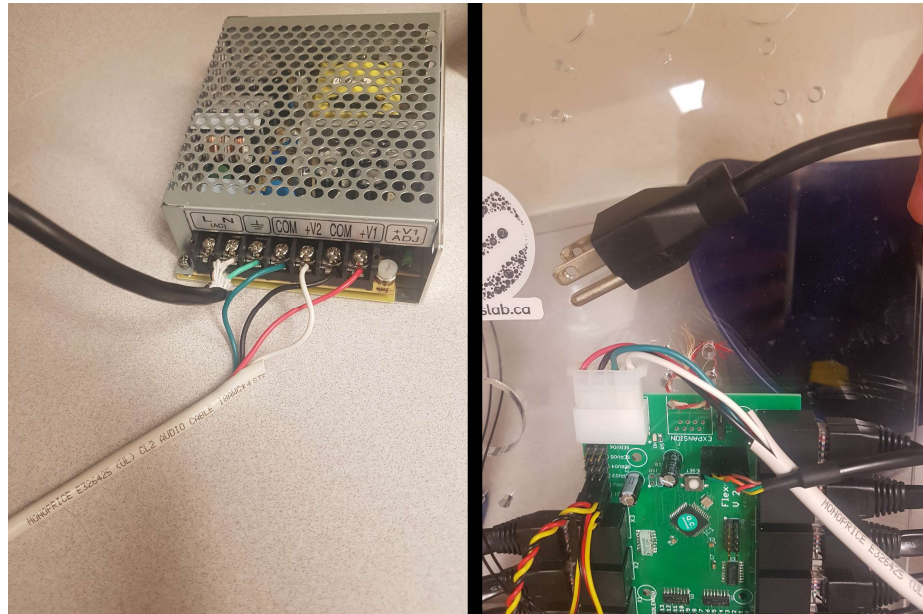


Figure 2.1.2.1: External power supply.
An external power supply is connected to the central PCB and power outlet.

2.1.3 Syringe pump

The media flow is aided by a custom syringe pump connected to the media source. The syringe pump consists of a servo motor connected to a sterile disposable 3 ml syringe (Air-Tite AL3) by 3D printed parts. The plunger of the syringe is pushed and pulled by the servo motor based on the amount of fresh media needed for each chamber. The amount of media pumped is determined by the optical density of the chamber and the threshold density set by the experimenter in the config.ini file ⁵⁸. Media will not be pumped into the chambers until the threshold density has been reached, at which point the syringe pump will

function to maintain that threshold optical density for the remainder of the experiment. This control loop feedback system is based on the proportional plus integral feedback controller⁵³. The proportional and integral gain parameters (k_p and k_i respectively) were chosen such that

$$rk_p^2/(4k_i) = 5 \quad (1)$$

Where r is the minimum allowable threshold OD, equal to 0.1. Since Equation (1) is greater than 1, oscillations about the threshold OD are prevented⁵³.

All 3D printed parts were printed using an Ultimaker 3. The filament material was acrylonitrile butadiene styrene (ABS), infill 30% with 0.2 mm resolution. All 3D printed parts connected by screws were first threaded with a 6-32 tap and lubricant.

A brass gear rack (McMaster-CARR) was cut to 95 mm in length and glued onto a 3D printed slide. This was fit into the 3D printed body of the syringe pump. A servo motor (Servocity, HS-645MG) was connected to the body using screws. A gear from the servo motor accessories was attached to the servo drive shaft to enable the slide to move back and forth. The plunger of the syringe was attached to the slide, while a final 3D printed part holds the syringe in place (Fig. 2.1.3.1). This allows the motor to push and pull the plunger of the syringe.



Figure 2.1.3.1: Syringe pump.

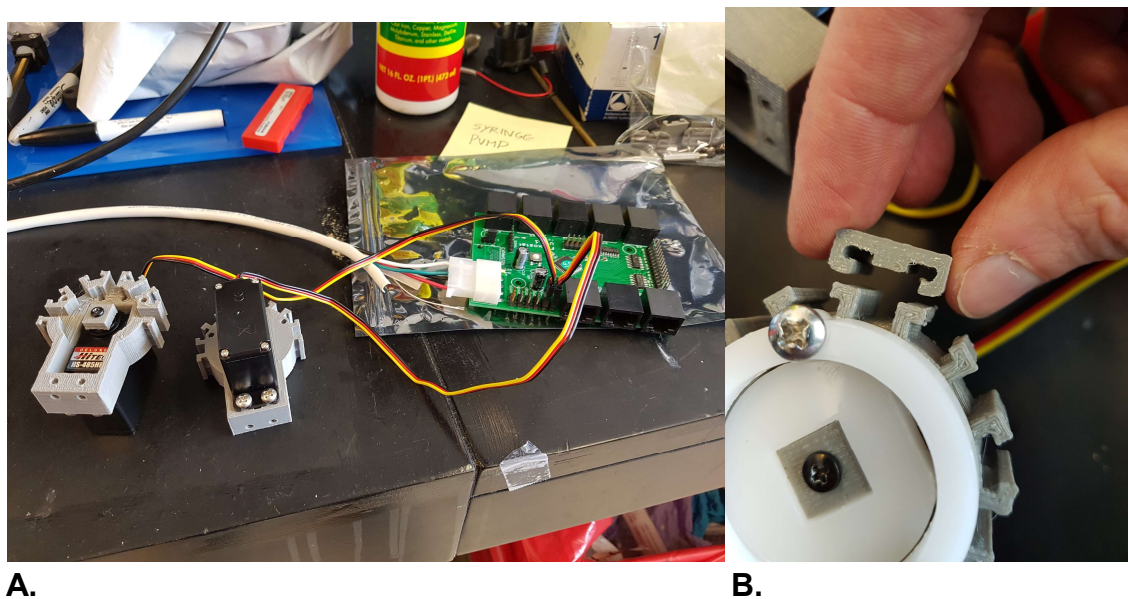
The servo motor rotates clockwise to uptake 0.1 - 1 mL, and dilutes by rotating counterclockwise. The degree of rotation (and therefore dilution) is determined by comparing the measured OD_{650} to the threshold OD_{650} .

2.1.4 Pinch valves

This turbidostat has eight chambers, meaning eight different experiments can be run in parallel. They are all connected to the media bottle by custom pinch valves as indicated by the black triangles in the schematic (Fig. 2.1.1). These pinch valves were built using servo motors, laser cut Delrin and 3D printed parts. The servo motors are controlled by the PCBs, and as they rotate, they in turn rotate a piece of Delrin that can pinch off any given chamber's media flow. Each chamber is continually cycled through for the duration of the experiment by the Python ⁵⁹ computer program servostat.py ⁵⁸ running on a laptop. Once every minute, optical

density readings are made for each chamber and outputted to a text file, along with the times of these readings, and their corresponding dilution rates.

Two identical pinch valves were built to control media flow from chambers 1-4 and chambers 5-8, respectively. The body of the pinch valve was 3D printed and screwed onto a servo motor. Vector files for the centre wheel and pinchers were sent to the online manufacturer Ponoko that laser cut the pieces out of Delrin. Delrin was used because it provides the strength needed for parts that incur repeated compressed force throughout an experiment. Eight clips were 3D printed to sandwich each chambers media tube between the Delrin pinchers and the 3D printed clips (Fig. 2.1.4.1). These pinch valves were attached to the central PCB that controls when they open and close. A valve opens when the servo motor rotates the centre wheel to the desired position, temporarily relieving the pressure on one media tube at a time and allowing media to flow into one chamber.



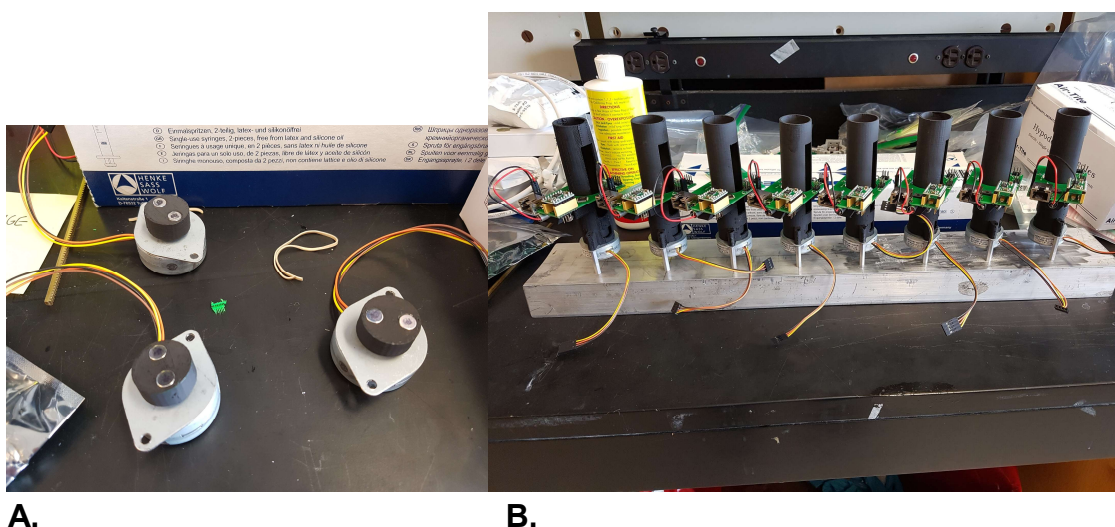
A. **B.**
Figure 2.1.4.1: Pinch valves.

A. Two identical servo motors attached to custom 3D parts are needed to separate the eight independent chambers. **B.** The white Delrin wheel is rotated by the servo motor to select the desired chamber to dispense media into.

2.1.5 Chambers

Chambers hold the test tubes, lasers, PCBs and stir bar motors together. Eight chambers were 3D printed to house eight separate (25 x 150 mm) test tubes. Each test tube holds a 32 mL volume. In order to stir the culture, magnetic stir bars (VWR Spinbar, 58949-006) are placed in each test tube and are rotated continually by a custom stir motor as follows. For one stir motor, a wheel was 3D printed with two holes on opposing sides into which small magnets of opposite polarity fit. Each wheel was pressed fit onto a stepper motor. Each chamber has one stir motor that is controlled by its PCB and rotates at 118 revolutions per minute (RPM). In this way, the stir motor continually rotates the wheel, which rotates the magnetic stir

bars in the test tubes above it (Fig. 2.1.5.1A). In order to keep the chambers stable each was attached to an aluminum block using standoffs and the PCBs were attached to each chamber. Each chamber was affixed with a light source that is read by the photodetectors. For this, 650 nm lasers (DigiKey, VLM-650-03-LPA-ND) were used and positioned to shine horizontally through each chamber's test tube (Fig. 2.1.2.1B). The ends of each laser were crimped and fed into a connector housing to attach them to the pins on the chamber PCB.



A. **B.**
Figure 2.1.2.1: Stir motors and chambers.
A. Magnets of opposite polarity are press fit onto a stepper motor. **B.** Printed chambers are attached on top of stir motors and held in place by an aluminum block. Chamber PCBs are slid on top of each chamber.

To get a better signal to noise ratio, approximately 10% of the laser's light is sent to the first light sensor before it is transmitted through the test tube solution to the second sensor. This initial reading before transmitting through the solution serves to normalize the measurements. To obtain the initial reading, the laser is

reflected at a 45° angle using a glass coverslip cut to 11 x 5 mm with a diamond cutter (Fig. 2.1.5.1).

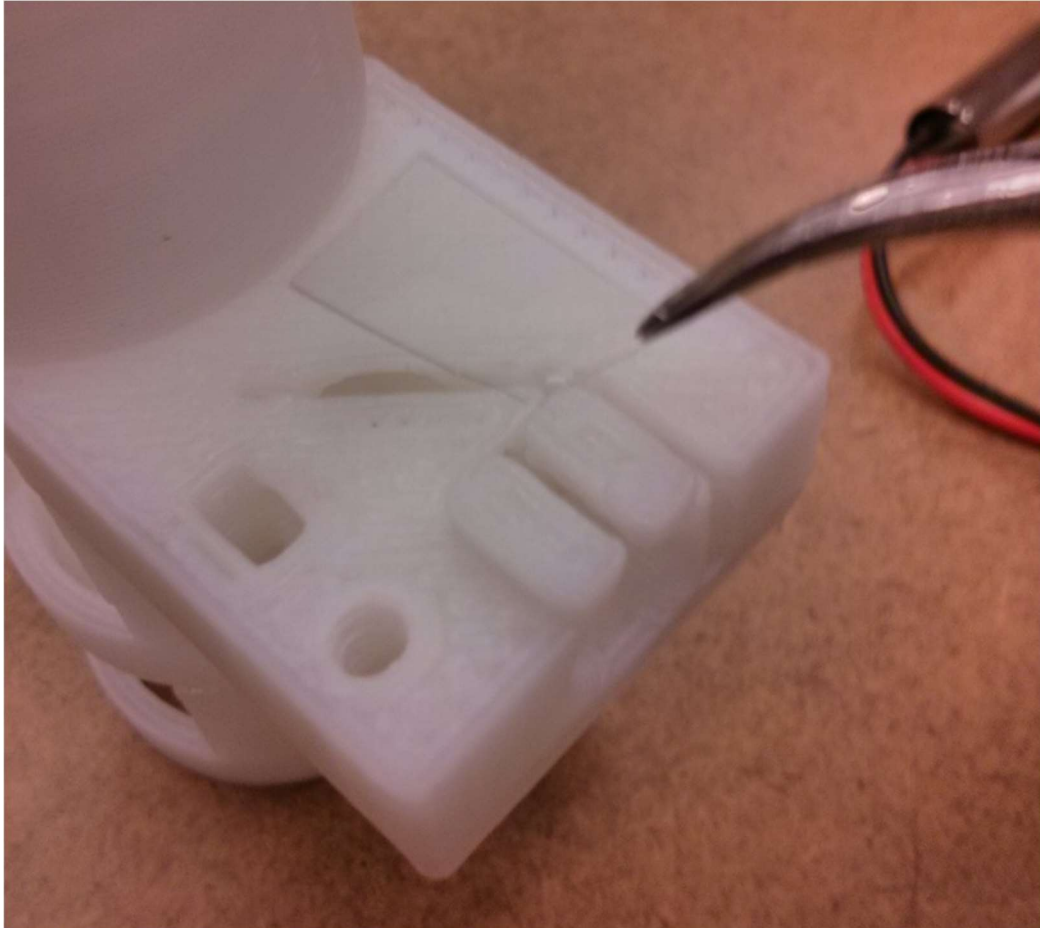


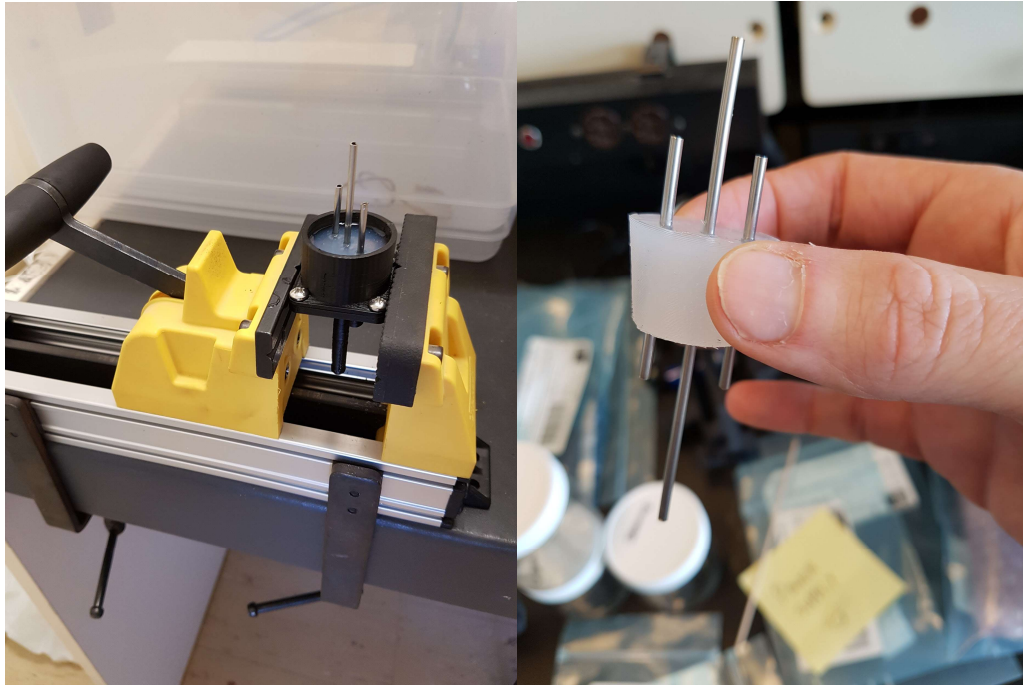
Figure 2.1.5.1: Glass coverslip ⁵³.

Glass coverslips are not manufactured small enough to fit into the chambers, they needed to be cut.

The chamber PCBs are connected to the central PCB via ethernet cables. Each chamber PCB calculates its optical density and relays it back to the central PCB. The central PCB controls the pinch valves for new media and the syringe pump for volume based on the optical density of each chamber.

2.1.6 Stoppers

To add fresh media and avoid overflow, each chamber is fitted with a custom three-piped stopper as shown in the schematic (Fig. 2.1.1). The leftmost pipe connects to the media source and allows fresh media into the test tube. Effluent can flow out of the chamber (mid pipe) because positive pressure is added from the right pipe. This pressure is created by attaching two aquarium pumps to syringe filters which pump sterile air into the chambers. Stoppers were custom made from silicone as follows: A mold for the stopper was 3D printed, three stainless steel pipes of outer diameter 2 mm and lengths 9, 4.5, and 4.5 cm were cut with a Dremel and secured to the mold. Two part silicone (Dragon Skin 30) was mixed together and poured into the mold, creating a solid silicone stopper less than 24 hours later (Fig. 2.1.6.1).



A.

B.

Figure 2.1.6.1: Stopper mold and final product.

These stoppers are autoclavable, and provide an airtight seal around the stainless steel tubes.

2.1.7 Software installation

Atmel Studio ⁶⁰, an integrated development platform was downloaded along with the programmed microcontroller .hex files ⁵⁸ to install all of the PCBs firmware by individually connecting an AVR programmer (DigiKey, ATATMEL-ICE-ND) to a laptop and each PCB. Python version 2.7 was installed with the necessary packages Numpy ⁶¹ and pySerial ⁶² in order to run the main program from a laptop which periodically measures the optical densities of each chamber and directs the microcontrollers to act accordingly (operate the pump and pinch valve systems) until the experiment is stopped. A free open source file transfer application PuTTY

⁶³ was installed which allows each chamber to be manually filled with media before starting an experiment.

2.2 Final Assembly

The syringe pump, pinch valves and central PCB were mounted to a 1x1 foot acrylic board. The central PCB was connected to an external power supply via a molex connector, to the eight chambers on the aluminum block via ethernet cables and to a laptop via a serial to USB cable (Sparkfun, FTDI cable). Test tubes with magnetic stir bars and stoppers were placed in each chamber. Silicone tubing (1/16 inch inner diameter, 1/8 inch outer diameter) was attached to each of the stoppers pipes. The silicone tubes attached to the media pipes are fed through the pinch valves up to a media reservoir. The tubes carrying air flow were connected to aquarium pumps, and the effluent tubes were connected to a waste container (Fig. 2.2.1).



Figure 2.2.1: Final Assembly.
This setup of the turbidostat is roughly 3 ft tall, 3 feet wide, and 3 feet deep.

2.3 Verification of Function

To test the proper functioning of the turbidostat, the first few experiments were conducted under ambient lab conditions. Cell growth dynamics were interrogated with one facultative anaerobic strain (*Escherichia coli* BL21) in Lysogeny Broth (LB) over three days. Optical density and dilution rates were automatically measured and recorded every minute of the experiment. Six of the

chambers (32 mL) were inoculated with 0.3 mL of an overnight culture of *E. coli* in order to determine the reproducibility of the growth curves. Two negative controls were included. The optical density threshold was set to 1.0.

2.4 Modifications to Improve Reproducibility

Modifications were made to the system to improve growth curve reproducibility between chambers. The original pinch valves were 3D printed from the .stl files located on the turbidostat's GitHub page ⁵⁸. The .stl files included two identical main pinch valve bodies and eight identical clips. Each pinch valve body controls four chambers. Hypodermic silicone tubes used as a media line for each chamber are suppose to be held in place on the main body by the clips. The space created for the clips to attached to the main body was too small (Fig. 2.1.4.1B), and the middle section of the clip was too short, unable to properly pinch the media line. Leaky pinch valves were suspected to be a contributing cause of chambers whose growth curves consistently lagged behind the others. By importing the original .stl file into a computer aided design (CAD) software (SolidWorks 2017 Student Edition) the dimensions of the pinch valves were adjusted (Fig. 2.4.1) to allow proper flow in the open position. They were widened based on the ANSI standard for engineering fit ⁶⁴. The fit type chosen was LT6, which is a locational transition fit where the hole and shaft diameter have negligible differences. Using this engineering fit the clip can be press fit onto the main body and secured in place. Widening the hole of the clips also loosens the pinching force on the media

tubes. The middle section of the clip was lengthened (Fig. 2.4.1) to increase the pinching force on the media tubes. Small incremental changes were made to lengthening the middle section of the clips and tested for their pinching abilities. If the middle section was too short then the chambers leaked media, if it was too long then the media was still pinched when it was supposed to be flowing in the open state. Excessive force was then applied in the closed state prematurely degrading the silicone tubing.

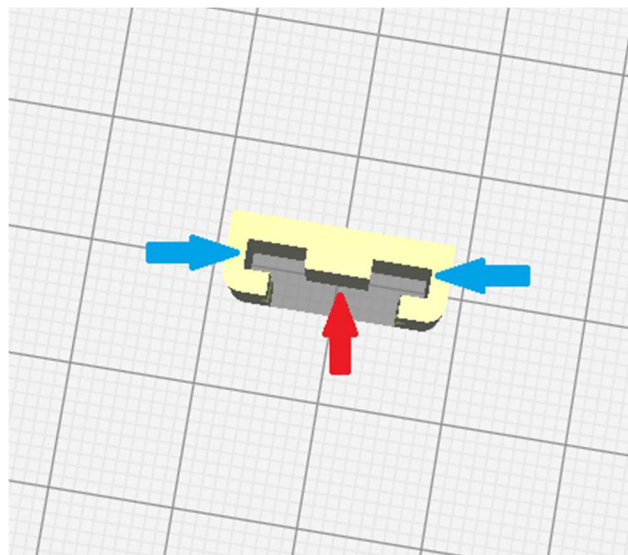


Figure 2.4.1: Pinch valve redesign.

The fit was adjusted to the LT6 standard by changing the dimensions of the hole as indicated by the blue arrows. The middle section of the clip (red arrow) was lengthened to reduce media leakage.

Reproducibility issues can arise at many points of the turbidostat's assembly, as well as when conducting an experiment, therefore, the protocol for inoculating the turbidostat was changed. The original protocol involved running the system blank for one minute to get a reading of the baseline OD₆₅₀, then inoculating

by injecting a needle into each chamber while the system was running. This created a problem due to the way that effluent is taken out of the system. Before an experiment is run, each chamber is manually filled with media up to the effluent tube. The effluent tube then removes any extra liquid added to the system by means of positive pressure due to the air tubes pumping air into the chambers. When a chamber is inoculated with a given volume, that same amount of volume will immediately be removed through the effluent tube. The media removed is taken from the same place that the sample is inoculated, the surface of the solution. This means that a potentially large portion of the inoculum could be removed from the system, resulting in each chamber receiving a different initial concentration of microbes. These potential inoculation differences were mitigated by first inoculating with the aquarium pumps turned off. Each chamber receives the same amount of inoculate, which is dispersed evenly throughout the solution by letting the magnetic stir bars spin for 1 minute. Then the aquarium pumps are turned back on and the experiment is run.

2.5 Modifications to Increase Breadth of Experimental Design

The turbidostat chosen to be built was meant to culture single strains of bacteria under ambient lab conditions. Many modifications needed to be made in order for it to function under our experimental design.

2.5.1 Creating custom stir rates in the chambers

The magnetic stir bars in the original design spin too aggressively for sensitive bacteria to survive. Additionally, experimenters may want a flexible mixing rate, to control the interactions between community members. The mixing rate was changed from its initial and maximum rate of 118 RPM with a Python script that allows a defined RPM to be input by the user, the output of which produces an .EEP file which can be hardcoded to any chamber PCB using similar methods described when installing the PCB firmware. In this way, each chamber can have its own unique mixing rate.

Since the stepper motors under each chamber were designed to spin at 118 RPM, when a lower RPM is desired, the current sent to each motor needs to be decreased in order to avoid overheating. The current was decreased by tuning each PCB's current limit potentiometer, which has the ability to control and directly measure the voltage. Equation (2) relates the voltage measured to the maximum amount of current that is safely allowed to flow through the stepper motors coils.

$$V_{REF} = 8 * I_{MAX} * R_{CS} \quad (2)$$

The current sense resistance (R_{CS}) on the stepper motor driver is 0.050 Ohms. The reference voltage (V_{REF}) for the motor stepping at its max rate of 118 RPM is 160 mV. Turning the potentiometer clockwise or counterclockwise causes V_{REF} to increase or decrease respectively. By decreasing the voltage, a lower current

flowed through the coils which allowed the motor to step at a lower rate without overheating.

2.5.2 Improving footprint and data acquisition

The turbidostat needs to be connected to a computer for the duration of an experiment. The computer is used to start and stop the turbidostat, and store all of the optical density and dilution rates. A Raspberry Pi Zero (Pi) was used in replacement of a personal desktop/laptop. Without adding any additional peripheral devices to the Pi such as a mouse, keyboard or monitor, the turbidostat footprint was kept small, and its mobility increased. The Pi comes with built in WIFI, so it can be controlled by an external computer using remote access software. A protocol (Appendix I) outlines how to control the Pi with a personal cell phone.

During an experiment, the threshold optical density for each chamber can be controlled, as well as the ability to start and stop an experiment. Once an experiment is started, a log file is updated periodically writing the optical density and dilution rates of each chamber as well as the time each measurement is taken (once every minute). Another protocol (Appendix I) is used to obtain copies of the log files throughout an experiment. By sending these files to a personal laptop, the data of an ongoing experiment such as OD₆₅₀ and dilution vs time graphs can be analyzed, providing information on the progress of an experiment, and if any changes need to be implemented or the experiment terminated.

The basic Python script to produce a graph of OD₆₅₀ over time⁵⁷ was modified to interface with the statistical programming language R⁶⁵ in order to

create more detailed customizable graphs including dilution rates vs time and individual chamber OD₆₅₀ vs time graphs using the ggplot2 package ⁶⁶. A much needed legend was also added to identify each chamber's growth curve. The code implementing this is located in 9.0 Supplementary Materials.

2.5.3 Adding compatibility to 37°C environments

The temperature of the infant gut is 37°C and we want to replicate these conditions in a laboratory setting so these communities can be modeled more realistically. To achieve this, the 3D printed parts were re-printed with ABS, a material with a higher melting point than most other filaments, and the entire device was relocated to a 37°C walk-in incubator.

2.5.4 Adding compatibility to dry environments

In order to maintain the proper humidity, and avoid evaporation from the culture tubes, a humidifier was designed to increase the moisture in the air being pumped into the chambers (Fig. 2.5.4.1). An aquarium bubbler (Petsmart, Top Fin) was attached to the end of the air tube and submerged in a flask full of water.

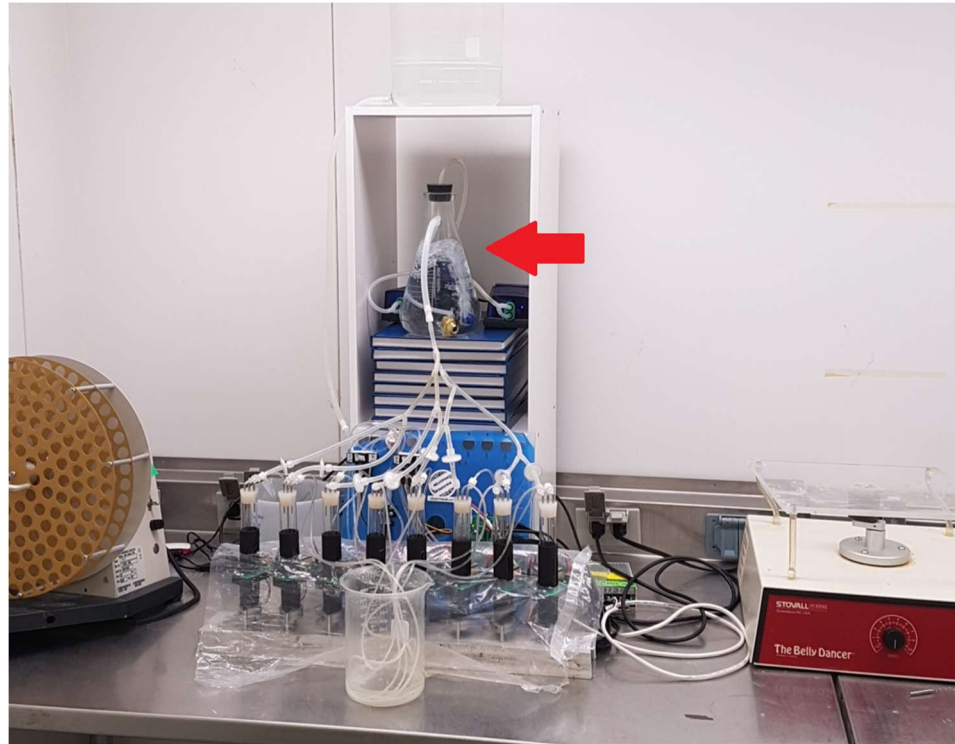


Figure 2.5.4.1: Humidifier.

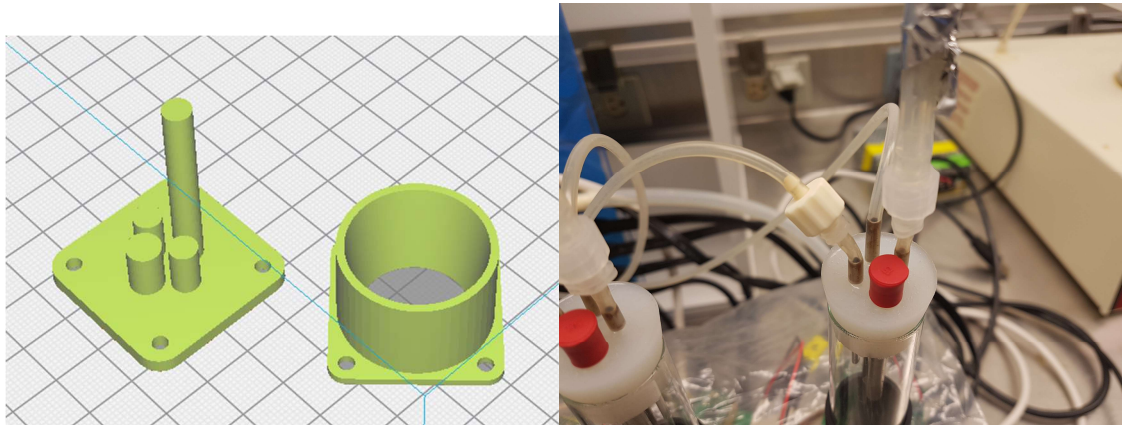
Indicated by the red arrow, the dry air from the aquariums pumps is hydrated with water before entering the chambers. This photo shows the turbidostat relocated to the walk-in incubator.

2.5.5 Adding compatibility to anaerobic environments

To maintain communities anaerobically, the turbidostat was placed in a controlled environment obtained by placing the effluent bottle and aquarium pumps inside of a 35 cu.ft bubble bag (VWR, 56616-258) with gloves and multiple ports to allow manipulation of the equipment. The bag was filled with nitrogen gas (N_2) and the system remained closed. N_2 was pumped throughout the chambers and back into the effluent bottle. The only sources of air leakage was from the media bottle and the chambers during sampling.

The original design of the media reservoir was a bottle with a spout at the bottom for media to flow out of. The cap on the media bottle needed to be slightly loosened, so that air can enter the bottle and help force the flow of media. To keep the media anaerobic, a sealed media bag (OMNI Medical Supply, SM1000) was used instead of a glass bottle. The bag remains closed during an experiment and collapses in on itself as the media leaves the bag. For anaerobic experiments, the reducing agent L-cysteine is added to the media to help remove oxygen ⁶⁷.

Under aerobic conditions, sampling from a chamber is performed by removing the stopper and pipetting. Using aseptic techniques ⁶⁸, no contamination occurs. For anaerobic experiments the stopper had to be redesigned (Fig. 2.5.5.1). A new mold was created to house an additional stainless steel pipe (4.5 cm in length, 5 mm outer diameter). A septum (Norell, SEPTA-5-R) was secured on it so that sampling can be done using a syringe needle.



A.
Figure 2.5.5.1: Stopper redesign.
A. CAD software is used to design a new stopper mold suitable for inoculation and sampling anaerobically. **B.** Culture is added or taken out of a chamber by piercing a septum with a needle.

Oxygen in the air was measured with a handheld oxygen sensor (AFC International, BWC2R-X) by placing it briefly into the enclosed bubble bag to give a coarse read of the oxygen levels in the system. In order to remove trace levels of oxygen, anaerobic sachets (Fisher Scientific, OXAN0025A) are stored in the bag and opened before an experiment starts. Since each sachet can only remove 2.5 L of oxygen, the bubble bag is deflated as much as possible, reducing its volume to a few litres. Four sachets are then opened to remove the remaining oxygen inside the bubble. Then, the nitrogen gas is turned on to fill the remaining volume of the bubble bag. Since this system is closed, very little nitrogen gas is used, just the initial filling of the bag.

2.5.6 Verification of function

A similar experiment to verifying the functionality under ambient lab conditions was performed to show that the turbidostat can work anoxically at 37°C. *Bacteroides thetaiotaomicron* (ATCC 12290), an anaerobic microbe⁶⁹, was grown anaerobically in ATCC meat broth with 15% glycerol for three days then normalized to an OD₆₅₀ of 1.0 using a plate reader (SpectraMax M3, 650nm). A 3 mL disposable syringe with corresponding hypodermic needle (Air-Tite, TSK SteriJect) was brought into the anaerobic chamber along with a sterile stopper. 3 mL of the culture was drawn into the syringe and corked with the stopper providing an anoxic condition for transferring the culture to the turbidostat. Six of the eight chambers were inoculated with 500 µL of culture by piercing each chambers septum with the needle. The media source in the turbidostat was Brain Heart Infusion (BHI) broth with 0.1% L-cysteine.

100 µL of the inoculum diluted in BHI + L-cysteine was serially diluted and the 10⁻⁵ dilution was plated on Tryptic Soy Agar with 5% sheep blood (TSA+B) in order to verify the purity of the culture before being used to inoculate the chambers. Two days after inoculation 1 mL samples were taken from the chambers by piercing the septum, drawing the chambers solution into a syringe and corking with a sterile stopper to be transferred back to the anaerobic chamber where 100 µL was serially diluted in BHI + L-cysteine and the 10⁻⁵ dilution was plated on TSA+B to verify that only our strain of interest has grown.

2.6 Culturing A Complex Community

A 0.1 g punch biopsy of a frozen infant stool sample (JCSA39) was serially diluted in BHI + L-cysteine and 100 μL of the 10^{-3} dilution was plated onto both MacConkey (MAC) and Columbia (CNA) + 5% sheep blood agar plates. The same method used in the *Bacteroides* experiment was used to anoxically transfer 3 mL of the diluted inoculum to the turbidostat. 200 μL was inoculated into six of the eight chambers. The media source was 0.2 BHI + L-cysteine + SCIMP (0.2 g/L Starch, 0.2 g/L Carboxymethyl cellulose, 0.2 g/L Inulin, 0.2 g/L Mucin and 0.2 g/L Pectin). 4.5 hours after inoculation, 1 mL samples were taken from each of the chambers using the same anoxic technique as described above and brought back to the anaerobic chamber. Four droplets from each sample were placed on pH strips (VWR, CA97027-086). Each sample was serially diluted in 0.2 BHI + L-cysteine and 100 μL of the 10^{-5} dilution was plated onto MAC and CNA + sheep blood agar plates. The rest of each sample was split into three aliquots. 300 μL was used for DNA isolation and sequencing of the 16S rRNA genes (Section 2.6.1), 700 μL was stored at -80°C for future studies (e.g., metabolomics). The same sampling, plating and storing method was then performed on all chambers 24 hours later.

2.6.1 DNA extraction and amplification for Illumina sequencing

Michelle Shah from the Surette laboratory isolated DNA from chamber samples using the method outlined in ⁴⁵. 300 μL of culture from each chamber was aliquoted into genomic preparation tubes containing 800 μL of 200 mM NaPO_4 , pH 8, and 100 μL guanidine thiocyanate-EDTA-N-lauroyl sarcosine. Samples were homogenized mechanically using 0.2 g of 0.1 mm glass beads (MoBio, Carlsbad, CA, USA). Samples were incubated at 37°C for 1 hour in 50 μL lysozyme (100 mg/mL), 50 μL mutanolysin (10 U/ μL), and 10 μL RNase A (10 mg/mL) to achieve enzymatic lysis. Samples were further incubated at 65°C for 1 hour in 25 μL 25% sodium dodecyl sulfate (SDS), 25 μL Proteinase K (20 mg/mL) and 75 μL 5M NaCl ⁴⁵. To extract DNA, supernatants were combined with phenol-chloroform-isoamyl alcohol (25:24:1; Sigma, St. Louis, MO, USA) and then purified with a DNA Clean and Concentrator-25 columns (Zymo, Irvine, CA, USA) using a vacuum manifold (EveryPrep Universal Vacuum Manifold, Life Technologies #K2111-01) according to manufacturer instructions. DNA concentrations were quantified using a spectrophotometer (Nanodrop 2000c Spectrophotometers, Fisher Scientific, #ND-2000C) and then stored at -20°C.

Another member of the Surette laboratory, Laura Rossi amplified the V3 region of the 16S rRNA genes of these samples with primers for Illumina high-throughput sequencing ⁷⁰. Approximately 200 ng of template was combined in a 50 μL reaction mixture containing 1.5 μL of 50 mM MgCl_2 , 200 μM dNTPs, 5 μL of 1 μM V3F_mod2 barcoded primer, 5 μL of 1 μM V3R primer, and Taq polymerase

(1.25 units/ 50 μ L PCR) (Invitrogen), amplified with the following conditions: 94°C for 2 minutes, followed by 30 cycles of 94°C for 30 seconds, 50°C for 30 seconds, and 72°C for 30 seconds, with a final extension of 72°C for 10 minutes. Amplified V3 16S rRNA gene products were sequenced at the McMaster Genomics Facility on a Miseq illumina sequencer (v2 2x250bp kit).

2.6.2 DNA extraction and amplification of contaminants for Sanger sequencing

While waiting for full community results from the inoculated chambers, the identity of the contaminants in the control chambers was determined by Aman Patel, an undergraduate student in the Stearns laboratory using the following methods:

To obtain crude cell lysis of contaminants for DNA sequencing, 100 μ L of the contaminated control was plated on CNA and incubated anaerobically for two days. Two colonies were picked into worm lysis buffer (WLB) with Proteinase K (Applied Biosystems) for DNA extraction. To make 50 mL of worm lysis buffer, Milli-Q water was combined with 2.5 mL of 1M KCl (Sigma-Aldrich), 0.5 mL of 1M Tris-Base (Sigma-Aldrich), 125 μ L of 1M MgCl₂ (Sigma-Aldrich), 225 μ L of Igepal (Sigma-Aldrich), and 225 μ L of Tween-20(Sigma-Aldrich). WLB reactions consisted of 50 μ L WLB and 2.5 μ L of 20 mg/mL proteinase K (Applied Biosystems). Colonies were incubated in WLB for 60 minutes at 56°C then the suspension was boiled at 95°C for 15 minutes to inactivate the proteinase K. Once finished, tubes with DNA were stored at -20°C until further use.

To identify the contaminant isolates, the 16S rRNA gene was amplified using the 27F and 1492R primers (IDT) ⁷¹. 5 μ L of DNA from the crude lysates was used as a template and combined in a 25 μ L reaction mixture containing 5 μ L 5X Standard PCR Buffer with MgCl₂, 0.5 μ L 10 mM dNTPs, 1 μ L 10 μ M 27F primer, 1 μ L 10 μ M 1492R primer, 1 μ L 10 mg/mL bovine serum albumin, and 0.125 μ L of 5000 U/mL OneTaq DNA polymerase (New England BioLabs). Reactions were amplified with the following conditions: 94°C for 5 minutes, followed by 30 cycles of 94°C for 1 minute, 56°C for 1 minute, 68°C for 2 minutes, with a final extension of 68°C for 10 minutes.

PCR products (1465bp) were separated through gel electrophoresis (1% agarose gel, 120V for 30 minutes) to ensure specificity. 20 μ L of each PCR product was then purified using the Monarch PCR and DNA Cleanup Kit (New England BioLabs) according to the manufacturer's outlined instructions. One modification to the manufacturer's protocol was that DNA was eluted in 10 μ L PCR water, instead of elution buffer. DNA concentrations were quantified using a spectrophotometer (Nanodrop 2000c Spectrophotometers, Fisher Scientific, #ND-2000C), and then sent for Sanger sequencing in the forward direction alone at the McMaster Genomics Facility (Mobix laboratory, Farncombe Institute, McMaster University). Genera and species of the isolates were identified by BLASTn alignment against NCBI's nucleotide collection ⁷².

2.6.3 Data analysis

Raw sequence reads were trimmed with cutadapt (v1.14; cutoff of 30 and minlength of 100) ⁷³ and then amplicon sequence variants (ASVs) were identified with DADA2 ⁷⁴.

The ASVs were imported into R and the vegan package ⁷⁵ was used for community ecology analysis. Microbial diversity within chambers (α diversity) was quantified by the Shannon diversity index ⁷⁶. The diversity reproducibility between chambers (β diversity) was quantified using the Bray-Curtis dissimilarity metric ⁷⁷. Species richness for each sample was estimated by rarefying the raw counts with a subsample size equal to the chamber with the smallest number of reads ⁷⁸.

3.0 RESULTS

The following results show that a custom continuous culturing device can be built to study the long term growth of microbes. Experiments involving individual microbes that prefer anoxic and 37°C conditions were grown and held at a constant OD₆₅₀ reproducibly, with the potential to increase the complexity of the community to that of an infant's stool sample. These capabilities now provide microbial ecologists with an additional tool to study long term community dynamics of previously difficult to culture microbes *in vitro*.

3.1 Validation of the original design

After the construction of the turbidostat was complete, the next aim was to validate the original design. In order to show that the turbidostat was functioning comparably to the original model, six of the chambers were inoculated with equal amounts of *E. coli*, while the remaining two chambers were left as negative controls. The initial optical density threshold was set to 1.0. The turbidostat was able to keep the *E. coli* in a continuous culture at an OD₆₅₀ of 1.0 for up to 72 hours without contamination (Fig. 3.1.1), at which point the experiment was terminated. Since the six chambers were inoculated with identical amounts of *E. coli*, it was expected that the growth curves would also be identical. The growth curves indicated, however, that the *E. coli* grew at different rates, as observed by the variations in optical density of the six chambers. These results implied that improvements to reproducibility were necessary; these improvements are outlined in Section 3.2.

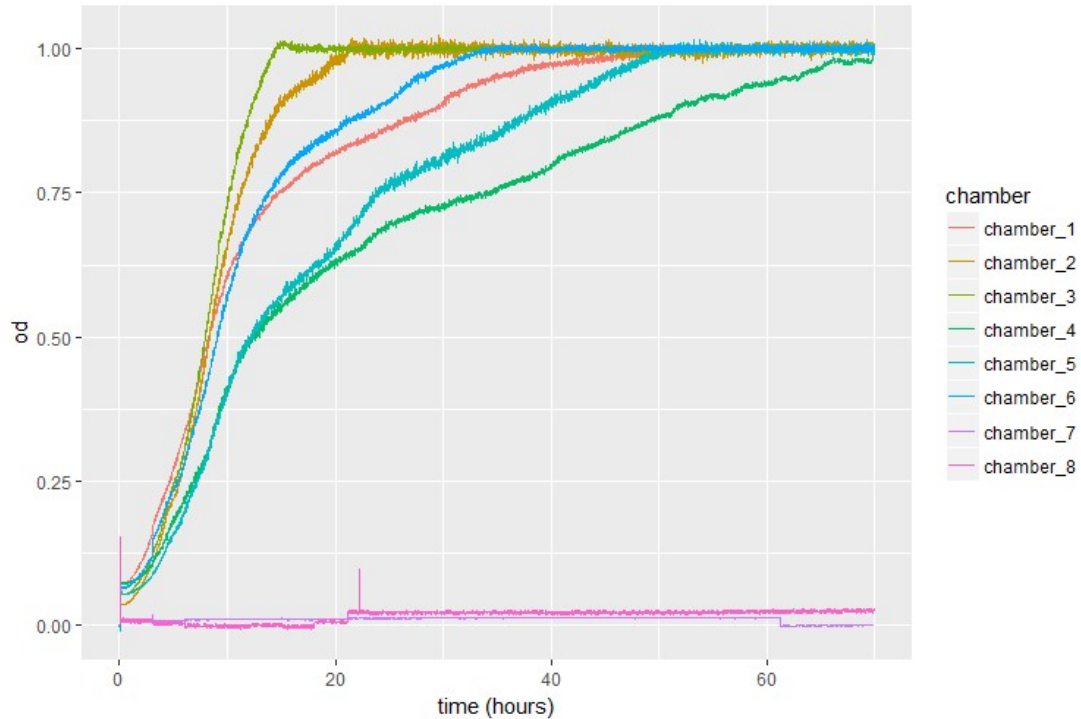


Figure 3.1.1: Optical density of *E. coli* BL21 over time. Chambers 1-6 were inoculated with 0.3 mL of overnight cultured *E. coli* and OD_{650} was set to 1.0. OD_{650} was measured every minute.

Dilution rates over time (Fig. 3.1.2) were analyzed to see if the syringe pump was functioning properly, and to gain insight into each chamber's stability at the threshold OD_{650} . The dilution rates recorded into the log file are pump units, where one pump unit corresponds to diluting approximately 1.5 – 2.5 μL of media. The minimum dilution rate is 7 pump units, as shown by the controls maintaining this rate throughout the experiment (the maximum dilution rate is 160 pump units). By choosing a minimum dilution rate of 7 pump units, dead communities will become apparent as they are slowly washed out, while having a negligible effect on a community's growth as it reaches the threshold OD_{650} . The syringe pump was operating appropriately, diluting only once the threshold OD_{650} was met. The faster

a chamber approached its threshold OD_{650} the higher the initial dilution rate was. The dilution rates remained variable at the threshold OD_{650} , opposed to the fix rate of chemostats. Although, each chamber's dilution rate had a range spanning 20 pump units, meaning all the dilution rates of a give chamber were within approximately 30 μL of each other.

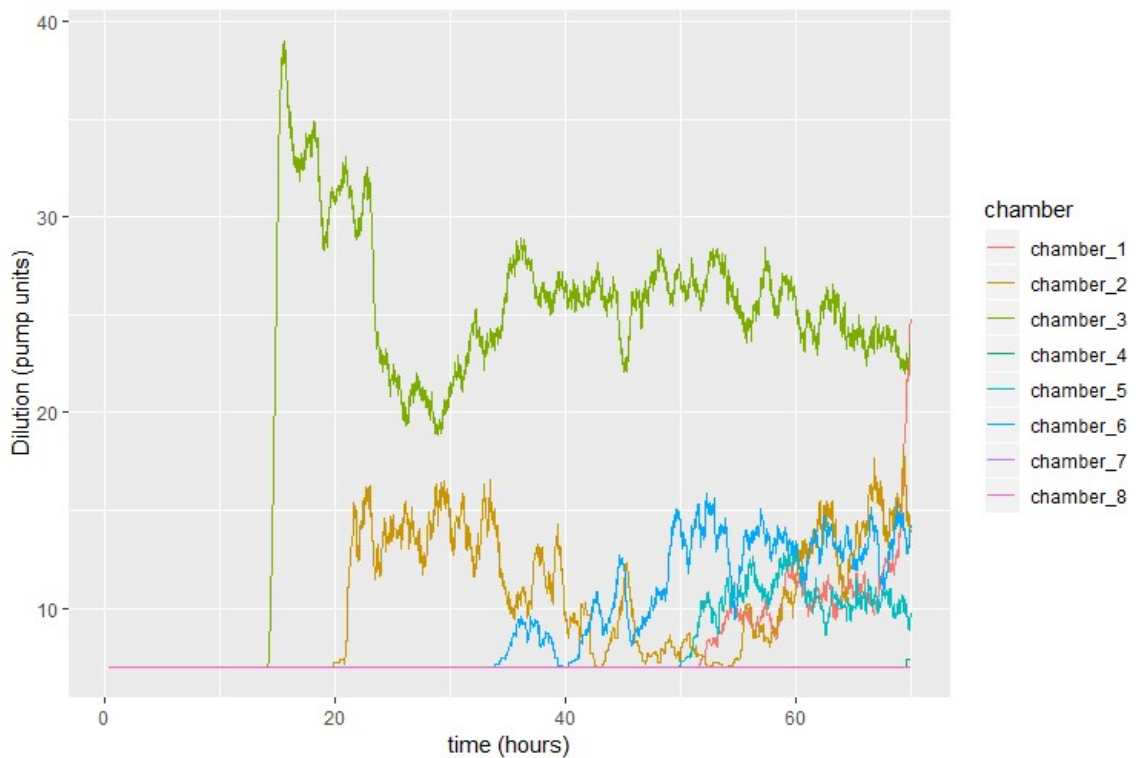


Figure 3.1.2: Dilution rate of LB over time.

The time points align with those from the optical density of *E. coli* BL21 over time (Fig 3.1.1).

To verify that the turbidostat was producing accurate OD_{650} readings, samples from each chamber of the turbidostat were taken to a commercial plate reader (SpectraMax M3, 650nm). This plate reader measures OD_{650} in a similar

way to the turbidostat, with the differences between readings being attributed to each device's individual way of reducing noise. Fig. 3.1.3 shows a linear relationship between the plate reader and the turbidostat for most chambers, indicating that these chambers were functioning properly. However, in chambers four and five the optical density read by the turbidostat was lower in comparison to all other chambers. Data points from chambers four and five were further from the regression line, thus indicating that technical issues needed to be addressed for these chambers. Given that these data points lie above the regression line, it is evident that the turbidostat's measured OD_{650} reading is lower than the actual OD_{650} . This accounts for why lower OD_{650} readings were observed in chambers four and five.

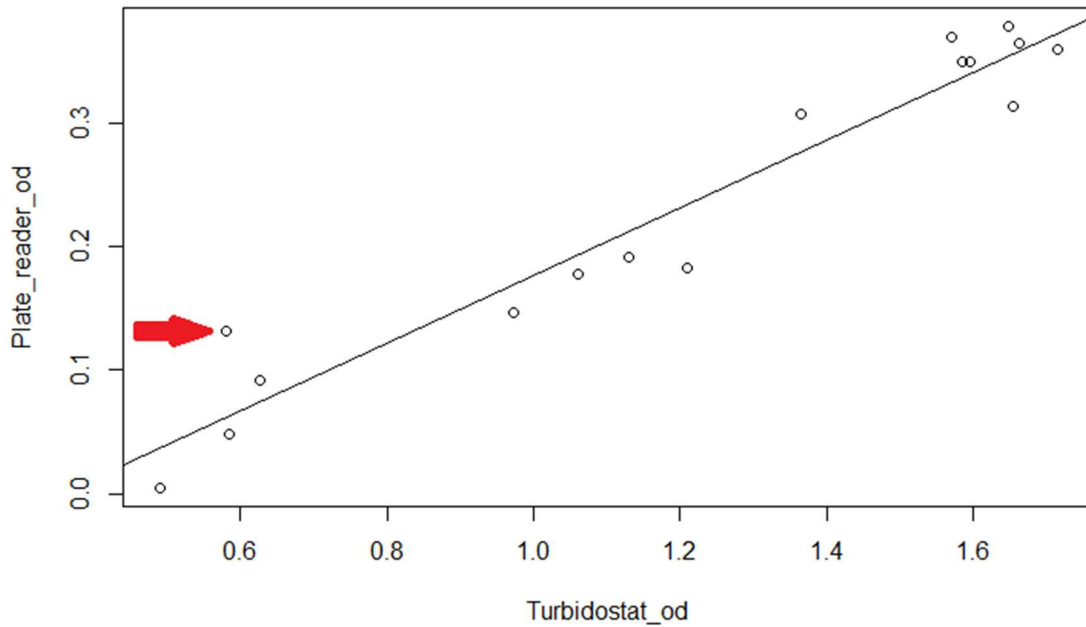


Figure 3.1.3: Commercial plate reader vs turbidostat.

These data points exclude chambers four and five. A perfectly linear relationship would imply the turbidostat's OD₆₅₀ readings are accurate. The difference in measured OD₆₅₀ readings from the regression line show the turbidostat is not completely reproducible across the chambers. The red arrow points to an OD₆₅₀ reading from chamber 6, another chamber that consistently lags behind the others. This is evident by the data point being far above the regression line.

3.2 Modifications to Improve Reproducibility

An important part of scientific experimentation is reproducibility^{79,80}. As mentioned in the previous section, OD₆₅₀ measured in chambers four and five were lower in comparison to all other chambers. All laser and light sensor lens were cleaned. Other factors could be contributing to the difference in growth curves, so modifications were made in an attempted to improve reproducibility between chambers.

3.2.1 Pinch valve redesign

One hypothesized cause contributing to the lagging OD₆₅₀ values was the pinch valves. If chambers four and five were too loose, extra media would leak into these chambers. Therefore, pinch valves were redesigned to ensure no media would leak in the closed position. The clip's hole length and width was increase by 2.75 mm and the middle pincher was lengthened 1 mm. With these changes, no leaking occurred in the closed position, yet media was free to flow in the open position.

3.2.2 Altering inoculation technique

The original inoculation technique was suspected to lead to different inoculum volumes being added to the chambers. Fig. 3.2.1.1 depicts the difference in growth curves between inoculating 1% and 0.1% of a chambers total volume with *E. coli*. The chamber inoculated with 10 times less volume took approximately 1.6 times longer to reach the threshold OD₆₅₀.

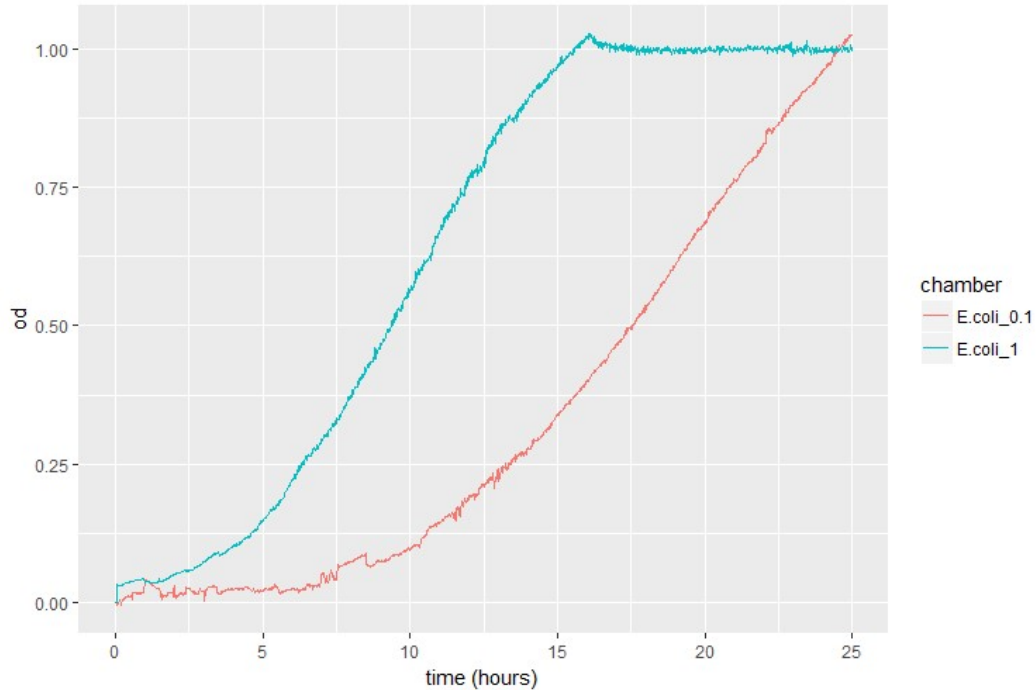


Figure 3.2.1.1: Different inoculate volumes.
OD₆₅₀ vs time graphs for *E. coli* inoculated with 1% and 0.1% of the chambers volume. The chamber inoculated with 0.1% took 1.6 times longer to reach the threshold OD₆₅₀ 1.0.

The new inoculation technique was performed as outlined in the methods section. By inoculating a low volume (< 2% of chambers volume) and starting the experiment one minute later, negligible differences in initial OD₆₅₀ readings were observed compared to the controls.

After the modifications to improve reproducibility were complete, an experiment was performed, similar to the experimental conditions in Fig. 3.1.1, where six chambers were inoculated with *E. coli* to test reproducibility. To quantitate any improvements in reproducibility, the sum of pairwise differences between absolute values of OD₆₅₀ between chambers was calculated. A value of zero would indicate that all chambers had the same OD₆₅₀ values over all the time

points, indicating they were identical. The larger the sum, the larger the differences in OD₆₅₀ readings between chambers. Implementing these modifications showed no quantitative improvements in reproducibility. Before the reproducibility modifications were made (Fig. 3.1.1), the sum of all pairwise differences between chamber's OD₆₅₀ values less than 0.6 was found to be 35. After the reproducibility modifications were made (Fig. 3.3.3.1), the sum of all pairwise differences between chamber's OD₆₅₀ values less than 0.6 was 42. As chambers four and five consistently grew slower than the others, they were designated to be the negative controls for all future experiments.

3.3 Modifications to Increase Breadth of Experimental Design

3.3.1 Custom stir bar RPM

In collaboration with Dr. Takahashi (University of Washington), user control of RPM was added with the python script `gen-prom.py`⁵⁸. `.eep` files were created corresponding to stepping rates ranging from 15-118 RPM. Turning the current potentiometer counterclockwise I was able to decrease the current by as much as half (for the 15 RPM case). This change eliminated overheating even when used at 37°C for over one week. Acceptable voltage levels were between 80 and 160mV since the RPM of the stepper motors was between 15 and 118 RPM (Fig. 3.3.1.1).

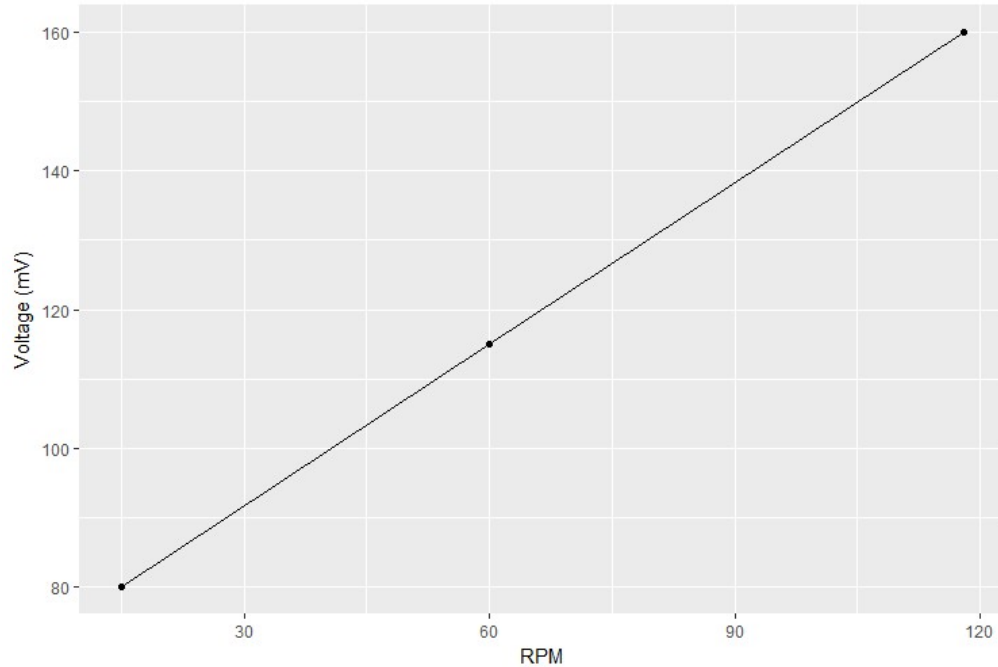


Figure 3.3.1.1: Voltage vs RPM

Acceptable voltage levels of the stepper motor driver given desired RPM of the stepper motor. RPMs of 15, 60 and 118 were interrogated.

3.3.2 Adding compatibility to dry environments

Inoculating *E.coli* into the turbidostat using LB as the media source in the 37°C walk-in incubator under aerobic conditions for two days led to some of the chambers volume decreasing by as much as 30%. The main cause of this evaporation was the hot dry air being pumped into the chambers. By pumping air through water before reaching the turbidostats chambers, I was able to humidify the air enough such that no evaporation was observed.

3.3.3 Adding compatibility to anaerobic environments

To determine if the turbidostat is capable of culturing anaerobic microbes, the anaerobic strain of *B. thetaiotaomicron* from ATCC was inoculated and its growth curve interrogated. Before an anaerobic experiment was performed, a plastic enclosure was filled with N₂ to reduce the amount of oxygen that the cultures were exposed to. Anaerobic indicators (Fisher Scientific, BR005B) were opened inside the bag that turned a faint pink colour indicating there was still trace elements of oxygen.

After rehydrating and plating *B. thetaiotaomicron* on TSA+B a single colony type was observed, one that was smooth, round and white and matching the ATCC description. As any media with blood cannot be used in the turbidostat due to its opacity, *B. thetaiotaomicron* was also grown in BHI. It became turbid overnight, proving BHI could be used as a media source for *B. thetaiotaomicron* in the turbidostat. A frozen stock made with 15% glycerol was thawed and plated on TSA+B and found to be pure.

Growth curves were produced (Fig. 3.3.3.1) from the experiment outlined in the methods section 2.5.6 where equal amounts of *B. thetaiotaomicron* culture were inoculated into six of the turbidostat's eight chambers using BHI as the media source.

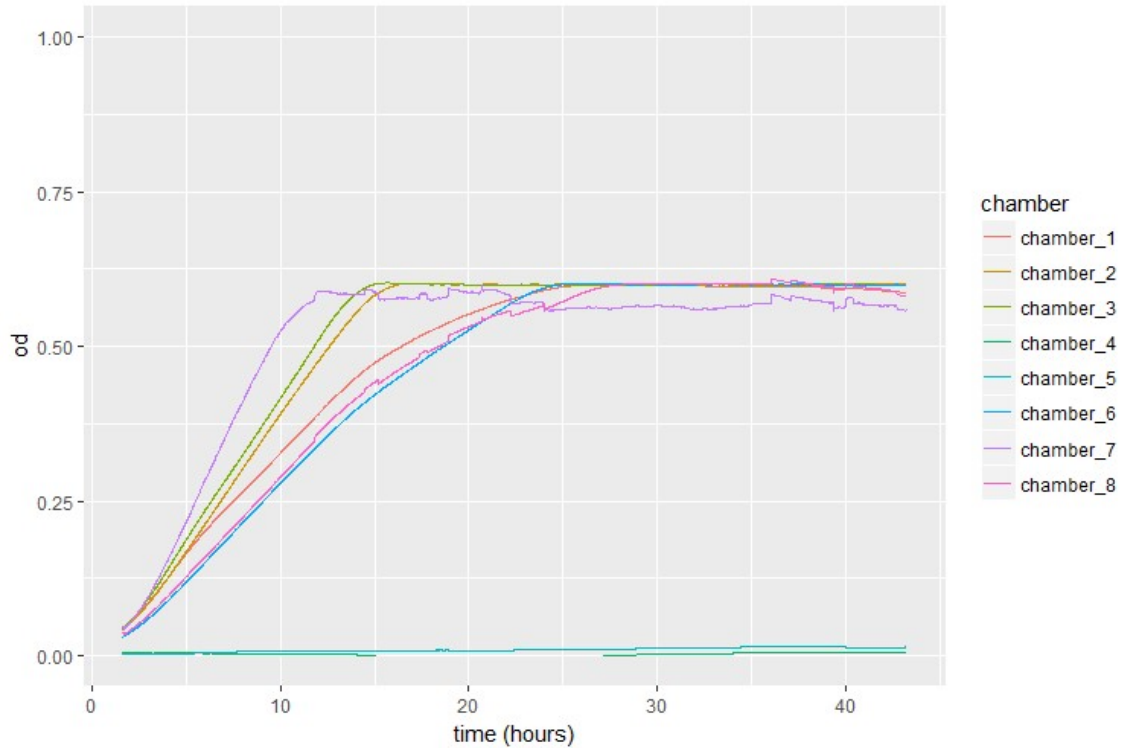


Figure 3.3.3.1: *Bacteroides* OD_{650} vs time. Proof the turbidostat can culture anaerobically. Chambers four and five are left as the negative controls. The threshold OD_{650} was set to 0.6.

Samples from the chambers were taken two days after inoculating and plated on TSA+B plates (Fig. 3.3.3.2). The same single colony morphology was observed without contamination.



Figure 3.3.3.2: Sample plated from the turbidostat.
A 100 μL sample is taken two days after inoculating the turbidostat with *B. thetaiotaomicron* and diluted to 10^{-6} and plated on TSA+B. This single colony morphology indicates *B. thetaiotaomicron* was cultured without contamination.

3.4 Inoculating a Stool Community

After the modified turbidostat was able to successfully culture an anaerobic microbe at 37°C, next we wanted to see how well we could recover the community of an infant stool sample, and how reproducible these communities would be between chambers. The original design of this experiment was suppose to run for two weeks, since it has been reported as the time needed for stool communities to stabilize in continuous culture ³⁶. Unfortunately, contamination was visible after 24 hours, and only two samples were taken from the chambers before the experiment was terminated. The first sample was taken 4.5 hours after inoculation, and the second sample was taken after contamination, at hour 28.5.

The original stool culture was plated onto both MAC and CNA plates as outlined in section 2.6. Eight distinct colony morphologies were observed on the MAC plate and two on the CNA plate (Fig. 3.4.1A,B). Frozen stocks were created from this culture with 10% skim milk. They were thawed and plated 24 hours later, producing similar morphologies seen on the plates from the original stool sample. This suggested that frozen stocks could be used for future experiments without the loss of any of the original community members.

Eight hours after the stool culture was inoculated into the turbidostat, samples were taken from each chamber and plated in the same way as the original stool culture. 70% of the colony morphologies from the original plates appeared. One colony morphology was absent from the CNA plates and two colony morphologies were not present on the MAC plates. Each chamber exhibited the same colony morphologies indicating that the chamber communities were similar to one another, and recouped most of the original community members. The second and final sample was taken 24 hours later, at this point 100% of the colony morphologies were observed (Fig. 3.4.1C,D).

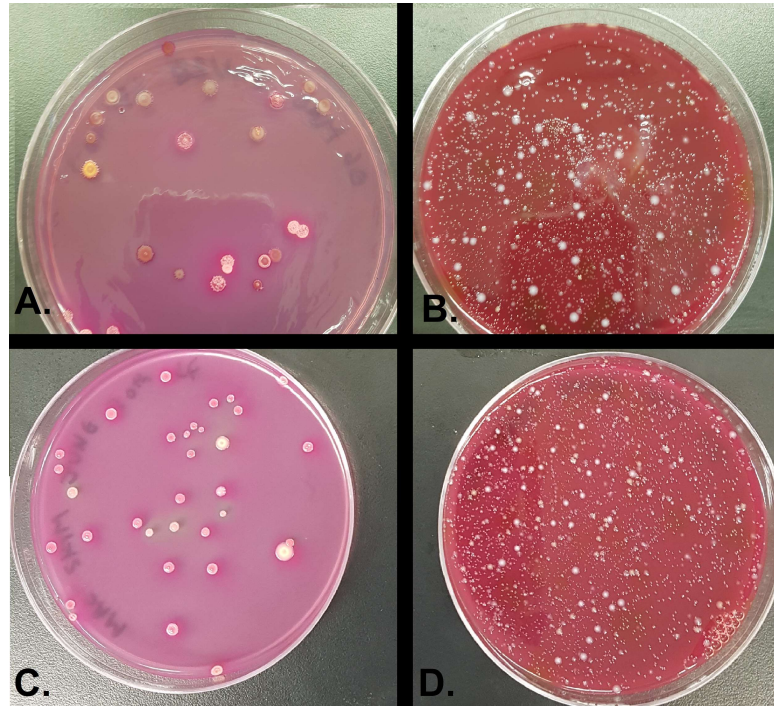


Figure 3.4.1: Stool community plated before and after turbidostat. **A.** MAC plate of stool community prior to inoculation. **B.** CNA plate of stool community prior to inoculation. **C.** MAC plate of second sample point. **D.** CNA plate of second sample point.

The sequence results from these time points were compared to the sequence of the original stool sample (Fig. 3.4.2) using stacked bar charts to visualize the relative abundances of ASVs.

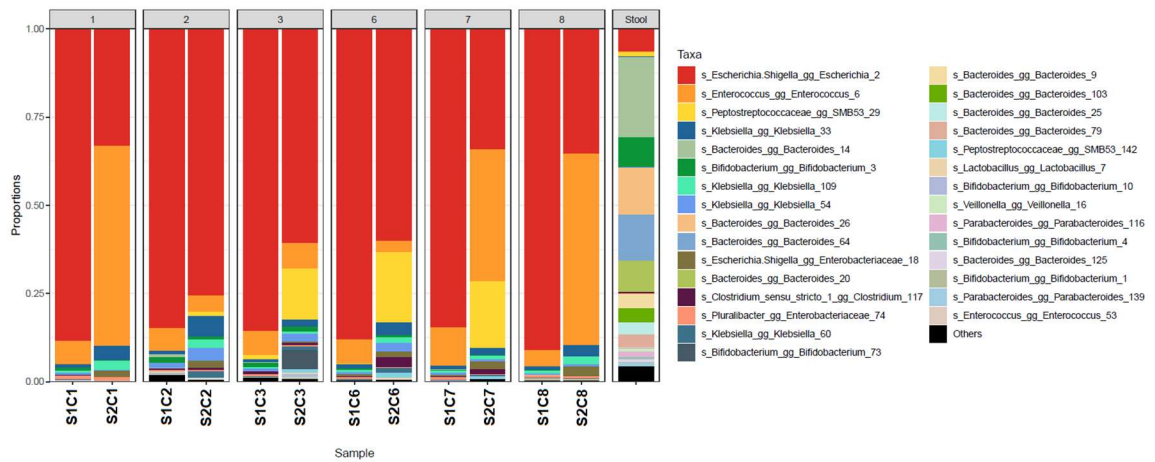


Figure 3.4.2: ASV relative abundances at each sample point. The x axis label S1C1 corresponds to the 1st sample of chamber 1. Each chamber has two stacked bar charts corresponding to the two sample points. The far right bar chart is the original stool sample.

The stool community was very different from the chambers, however, the chambers were similar to each other (Fig. 3.4.2). To quantify the diversity within each chamber a Shannon diversity index was plotted for each chamber at each time point. Diversity within each chamber increased with time (Fig. 3.4.3), however, after 28.5 hours the diversity had not reached that of the stool community.

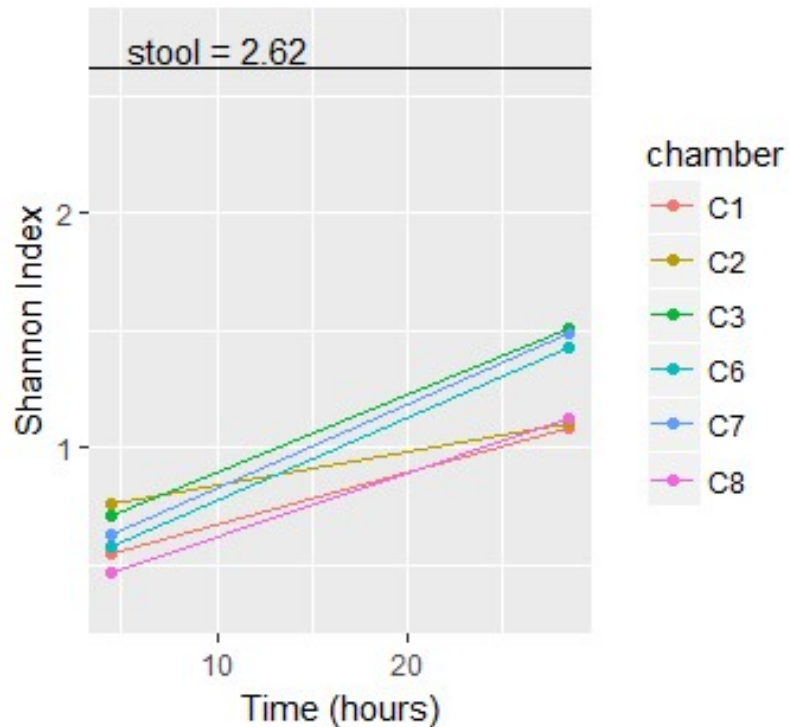


Figure 3.4.3: Shannon diversity index over time. The chambers are increasing in diversity over time, but after 28.5 hours in the turbidostat they have not yet reached the complexity of the original stool sample as indicated by the black horizontal line.

To quantify the chambers reproducibility, a Bray-Curtis dissimilarity box plot (Fig. 3.4.5) was created. A value of one corresponds to completely different samples, whereas a value of zero corresponds to samples with identical community composition. Both the samples taken at hour 4.5 and 28.5 were very different from the stool sample as seen by the second and fourth box plots. The chambers after 28.5 hours seem to be diverging in their microbial composition, compared to those after 4.5 hours, suggesting that the communities were becoming more dissimilar to each other over time.

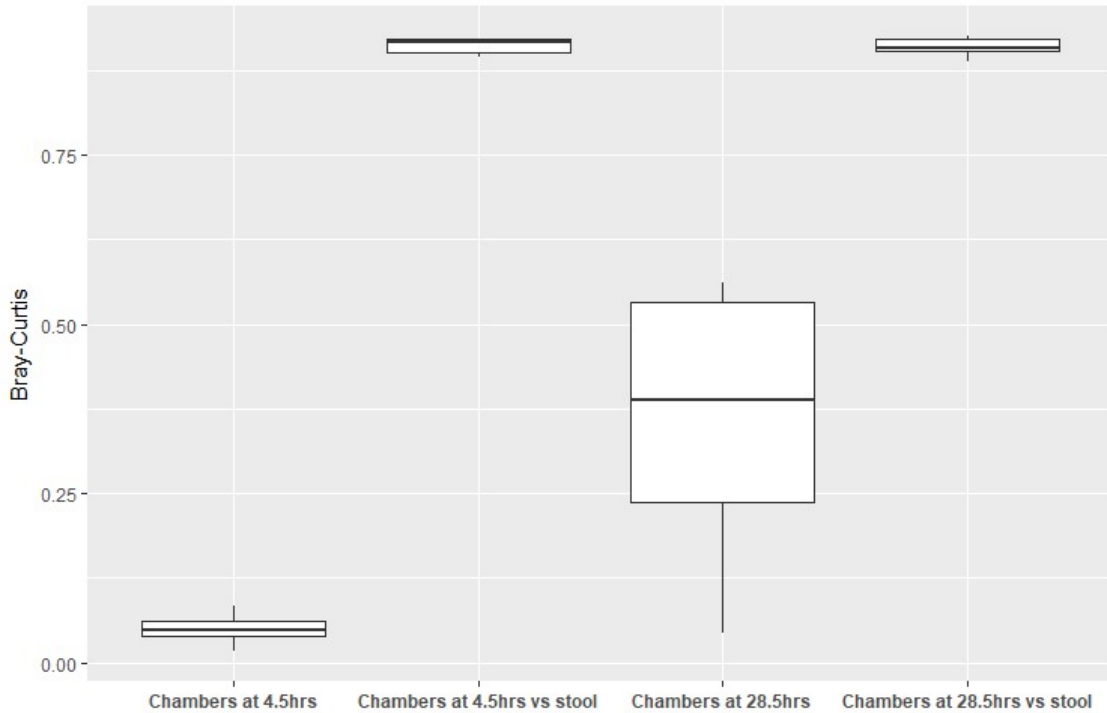


Figure 3.4.5: Measuring the Reproducibility of Diversity.

The Bray-Curtis dissimilarity metric is used to quantify the difference between chambers diversity at each of the sampled time points. The chambers diversity at each time point is also compared to the original stool samples diversity.

Relative abundances of the five most abundant phylotypes (ASVs) from the chambers were plotted over time (Fig. 3.4.6). Most phylotypes seemed to exhibit the same directional change in relative abundance except for *Enterococcus_6*, which was hypothesized to be the microbe that contaminated the controls and media source, leading to the termination of this experiment. The identity of the contaminant was determined by obtaining an isolate from the contaminated chamber and sequencing the full-length 16S rRNA gene (Section 2.6.2), which matched Genbank sequences for *Enterococcus faecium* or *Enterococcus durans* identified with BLAST. This increase in relative abundance from less than 10% to greater than 40% after 24 hours, while other chamber's levels remained less than

10% show the effect of contaminated media. It makes sense that chambers one, seven and eight exhibited the largest amount of contamination as their media lines were closest together. It is hypothesized that *Enterococcus_6* was able to use the condensation inside the chambers to climb up to the media inlet ⁸¹. All media inlets are connected to each other and to the media reservoir. Once one media inlet was contaminated, all chambers would eventually be diluted with contaminated media.

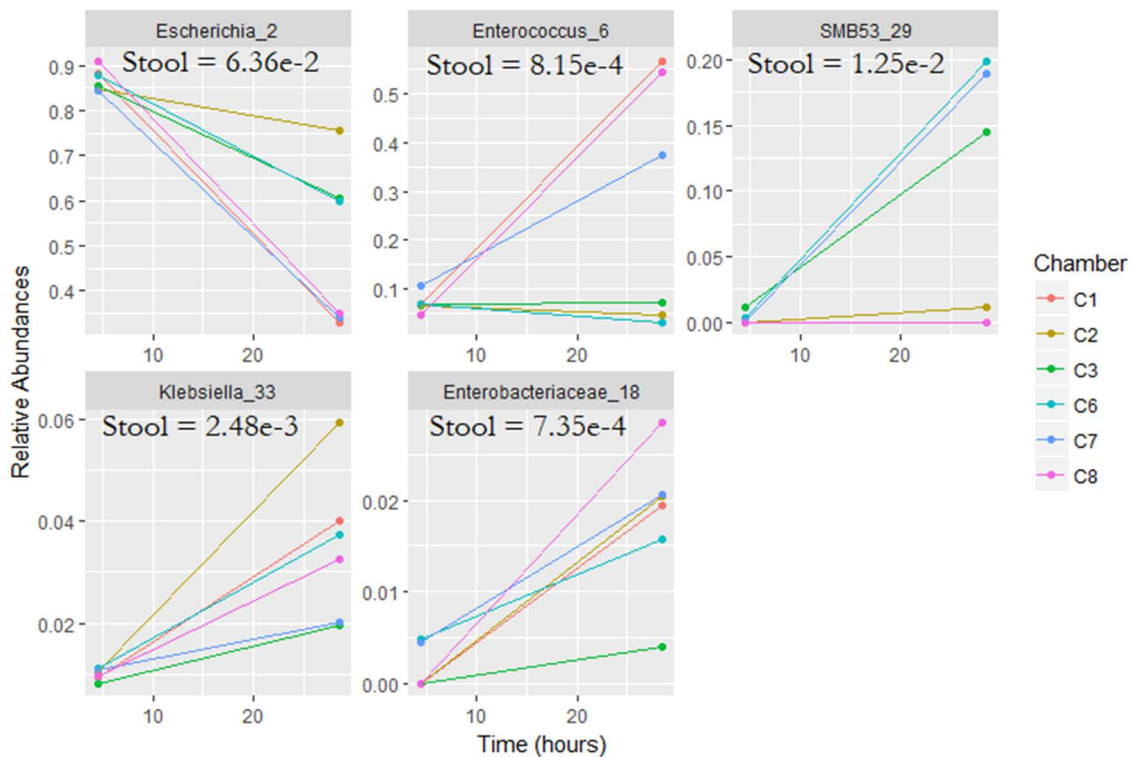


Figure 3.4.6: The five most abundant bacterial phylotypes (ASVs) over time. Most phylotypes exhibit the same behavior over time, except for *Enterococcus_6* which was contaminating the chambers at different time points. The original stool community contained all of these species, but in low abundances.

The average number of detectable phylotypes over all the chambers at hour 4.5 was 23, and at 28.5 hours that number increased to 25. The stool community

had 62 detectable phylotypes. 70% of the 23 phylotypes found in the chambers at hour 4.5 were also found in the stool. 66% of the chamber phylotypes at hour 28.5 were found in the stool. This means the chambers recovered 26% of the total stool community phylotypes. Though this percent coverage did not change over time, the phylotypes that comprised this number did. Some stool phylotypes did not show up in the chambers until the second time point. Other stool phylotypes present in the initial chambers failed to record any counts after 28.5 hours. The colony morphology counting, predicting the coverage of stool phylotypes in the chambers, overestimated the amount of the community that could be grown in continuous culture *in vitro*. 70% coverage was predicted at the first time point, whereas 100% coverage was predicted at the second time point. Comparing the sequencing results revealed 26% coverage at both time points. This perceived increase in coverage could have been due to an increase in phylotypes that have similar morphological traits to the stool community members that were not seen in the plates at hour 4.5.

To get a better estimate of the species richness, the raw counts were rarefied with a subsample size equal to the chamber with the smallest number of reads (1,902). In this case the average species richness at hour 4.5 was 18, and that increased to 19 by hour 28.5. The stool sample species richness was estimated to be 47 by this method.

4.0 DISCUSSION

Studying complex communities of microbes from a dynamic perspective presents a variety of challenges. Though there have been advances in the use of continuous culture devices to study microbial interactions, there are many limitations associated with their usage. In addition to the high costs of these commercial devices, one of the key disadvantages is the inability to run more than a few parallel experiments at the same time ^{51,52}.

In this project, I have utilized the framework published by Takahashi et al. and developed a cost-efficient turbidostat that is optimized to study bacteria in anoxic conditions at 37°C. Unlike conventional devices, that encompass only a small number of chambers ^{48,54}, the designed turbidostat enables eight separate experiments to be conducted in parallel, including two negative controls.

4.1 How Commercial and Other Custom Devices Compare

This modified turbidostat was built for under \$4,000 CAD, considerably less than other custom made or commercial continuous culture devices ⁵⁵. As most of these parts were ordered in bulk, building a second turbidostat would cost less than half of this.

Most custom made and commercial continuous culture devices are chemostats because their mode of media delivery is the least complex ⁸². One downside to these systems are their lack of real time interpretability. Some parameters can be continually monitored such as temperature and pH, but these can be monitored in turbidostats as well. Improving the turbidostat's data

acquisition and visualization improved the troubleshooting capabilities and provided more insight into the community dynamics. Having the ability to monitor the optical density within individual chambers and the dilution rates in real time allowed me to pinpoint any problems with contamination or media leakage. By plotting the OD_{650} over time of control chambers, I was able to determine when contamination occurred ($OD_{650} > 0$). If all of the chambers suddenly rise above the threshold OD_{650} , either the media ran out, the media became contaminated, or the syringe pump broke. If one chamber's growth is lagging behind another, but their dilution rates are the same, there could be some media leakage. These observations were helpful in determining the source of the problem, leading to a faster real-time solution and allowing an experiment to continue or to be discontinued as appropriate.

Dilution rate over time can also give insight into community dynamics. Once all the chambers were held steady at their threshold OD_{650} , visualizing a graph of the dilution rate over time gives us information about the composition and stability of the communities. Chambers being diluted at the max rate may have a different composition of microorganisms than the chambers being diluted at a slower rate. If the dilution rates are sporadic then the community may be less stable than others with a constant dilution rate. Most commercially available continuous culture devices suitable for laboratory experiments cannot provide these additional insights as their dilution rates are fixed.

4.2 Contamination Issues

The main issue stopping this turbidostat from future experiments with complex communities was contamination. Humidity problems arose when inoculating with different microbes under different environmental conditions. Experiments with *E. coli* under aerobic and room temperature conditions did not have humidity or contamination issues. During experiments with *E. coli* at 37°C and anaerobic conditions, the media inside the chambers evaporated due to the hot dry air being continuously forced onto its surface by the aquarium pumps. Adding the humidifier provided enough moisture to the air being blown such that the evaporation issues were alleviated.

Growing *Bacteroides thetaiotaomicron* (ATCC 12290) anaerobically at 37°C produced too much humidity, likely because of gas produced during fermentation⁸³. The chambers became too humid, condensation lined the inside of the chambers and the stainless steel pipes and clogged the syringe filters. Since no air was being forced into the chambers, no pressure was able to pull the effluent out of the chambers. Yet media continued to be added to these chambers, leading to an overflow out of the test tubes. Removing the humidifier from this experiment was hypothesized to reduce the condensation enough for the syringe filters to function properly, but the moisture produced by the fermentation process alone was enough to clog the filters again. In an effort to solve this problem syringe filters were removed and the system cycled N₂ from the bubble bag through each of its chambers to see if any contamination would occur by not sterilizing the air. The

experiment was stopped after three days as no contamination occurred, all previous experiment's contamination occurred within the first 24 hours. The same experiment was set up again, but this time *Bacteroides* was inoculated. The chambers and air tubes produced a lot of condensation, but the chambers did not overflow with media because there were no syringe filters to clog. The experiment was stopped after three days as no contamination occurred.

When a stool community was inoculated under similar conditions to the successful *Bacteroides* experiment, condensation again formed in the chambers and air tubes. An OD₆₅₀ vs time graph indicated that contamination had occurred of the controls near the 28 hour mark. At the 15 hour mark chambers one, seven and eight increased past the threshold OD₆₅₀ suggesting that the media source was contaminated. This led to the hypothesis that motile members of the community were using the condensation inside the chambers to travel up to the media inlet, contaminating the media source ⁸¹.

The *Bacteroides* experiment did not run into contamination issues because this organism is non-motile ⁸⁴. The contaminated controls from the stool community experiment were identified as *Enterococcus durans* and *Enterococcus faecium*, two microbes found in the human gut ⁸⁵. This strengthens the argument that the contamination was caused by the community inoculated and not from some outside source of contamination. Due to these contamination issues, successful experiments running anaerobically at 37°C were limited to those inoculated with non-motile microbes. A simple solution to this has been proposed in the future

directions section which should allow for any microbes to be cultured without contamination.

4.3 Future Directions

4.3.1 Reproducibility

In order to utilize all eight chambers, the reproducibility of these experiments must be improved. The source of variability between chambers should be interrogated in further detail. Laser and sensor lens were cleaned. Laser connections were taken apart and crimped tighter. This improved the signal to noise ratio but not the reproducibility. Lasers were switched between chambers to see if they were the source of OD₆₅₀ reading error, but no differences were observed. With all the adjustments made, the same chambers seemed to produce lagging results. The next step is to generate more data points for Fig 3.1.3, by measuring a sample's OD₆₅₀ using the turbidostat and a commercial plate reader. It is suspected the chamber's OD that consistently lag are due to slight misalignments in the laser sensors. These misrepresentations in OD₆₅₀ can be adjusted and normalized based on the difference found between them and the commercial plate reader.

4.3.2 Contamination

To stop motile bacteria from being the source of contamination, syringe filters could be placed on the media inlets of each chamber. Even if a chamber produced condensation with motile bacteria, they would not be able to travel back up the media line ⁸⁶. A syringe filter would need to be found that could allow the media to pass into the chamber by the force of the syringe pump, without creating too much resistance to overheat its motor. If such a filter does not exist a small portable humidity controller known as a hygostat ⁸⁷ can be purchased for under \$120 CAD and put inside the bubble bag. This device would be able to control the air's moisture inside the bubble bag such that evaporation or condensation issues would not occur in the chambers.

4.3.3 Future experiments

With the contamination issues from motile bacteria fixed, long term experiments can be performed with complex communities. Strategic changes to the environment could then be implemented to observe how the community responds. For example, the source of fiber could be changed to see how the communities composition and metabolites respond ⁴⁷. Eventually these observations could lead to the controlled ability to produce desired community compositions and metabolites. These experiments could be performed on a variety of communities with varying levels of member complexity, to show how interactions change as members are added or taken away.

5.0 LIMITATIONS

5.1 Limitations of This Turbidostat Design

This turbidostat has many continuously moving complex parts. Most of the parts have been built from very basic materials. The complex parts could have been purchased commercially, for example, commercial pinch valves could have replaced the 3D printed ones or peristaltic pumps could have replaced the need for pumping air into the chamber to remove the effluent ⁵⁵. But the main appeal to this system is its cost effectiveness and replacing these parts would easily double the cost of the entire turbidostat. The problem with using custom made parts comes down to reliability issues. The original design had not been rigorously tested under harsh conditions or engineered to sustain long term experiments ⁵³. The motors for the pinch valves and syringe pumps fail randomly. Media can dry in the effluent tubes from the continuous force of hot air, clogging the tubes and overflowing the chambers. The system must be monitored constantly, which can be a challenge with longer experiments.

Another limitation is the media source. Although each chamber houses an independent experiment, they all have to use the same media source. It would be useful to run experiments with different media types as outlined in the future experiments section, but this is not possible with the current setup as there is only one syringe pump operating all the chambers. To add the ability to customize the media for each chamber, eight syringe pumps would be needed and a new design of the central PCB as well as the software controlling the syringe pumps.

Although the mixing rate can now be customized prior to an experiment, once that rate is set it is fixed for the duration of the experiment because the stir bars are constantly rotating. Having the ability to vary the mixing rate throughout an experiment, including completely stopping the mixing could lead to many useful experiments. Spatial diversity is an important factor for many ecosystems ^{88,89}, but this cannot be studied as the chamber's solution is constantly stirred to maintain a homogenous mixture. If the ability to start and stop mixing was available, microbial ecology theories such as the intermediate disturbance hypothesis could be tested ⁹⁰.

Although the solution is constantly mixed, its rate could be set low enough to produce species gradients ⁹¹. For example, anaerobic microbes may be concentrated at the bottom of the test tube ⁹². Unfortunately there is no commercially available syringe needle thin and long enough to pierce the chamber's septum and reach past the surface of the solution. All sampling is done at the surface of the solution, meaning any microbes dwelling at the bottom of the test tube cannot be sampled.

Other limitations to this turbidostat are inherent to all turbidostats as outlined in the introduction. Light needs to be able to transmit the solution. This means certain opaque media types or high density growth rates cannot be accurately measured ³⁴.

6.0 CONCLUSION

A basic turbidostat designed to culture single microbes at room temperature and aerobic conditions has been customized to culture notoriously difficult microbes under more harsh conditions. Obligate anaerobes can now be grown at 37°C, with complex communities and moist environments likely possible with the simple addition of a syringe filter in the media line. Ease of sampling was improved with a stopper redesign that allows quick sampling straight from each chamber while maintaining anaerobic conditions. Monitoring ongoing experiments was improved with the ability to visualize growth curves in real time. All these achievements were built with the same cost-effective mentality that made the original design so appealing. A personal desktop/laptop used to run the system was replaced with a \$50 CAD Raspberry Pi. Anaerobic conditions ordinarily require the use of an anaerobic chamber, a specialized piece of equipment that costs tens of thousands of dollars. Here an anaerobe was cultured by using a reusable \$70 CAD bubble bag.

In conclusion, a more robust, easier to sample, monitor and diagnose turbidostat has been created. Many more experiments can now be interrogated with the ability to culture in extreme conditions. All of this was achieved for not much more than it cost to build the original turbidostat.

7.0 REFERENCES

1. Konopka, A. What is microbial community ecology? *ISME J.* **3**, 1223–1230 (2009).
2. Cho, I. & Blaser, M. J. The human microbiome: at the interface of health and disease. *Nat. Rev. Genet.* **13**, 260–270 (2012).
3. Tsiknia, M., Paranychianakis, N. V., Varouchakis, E. A., Moraetis, D. & Nikolaidis, N. P. Environmental drivers of soil microbial community distribution at the Koiliaris Critical Zone Observatory. *FEMS Microbiol. Ecol.* **90**, 139–152 (2014).
4. Bar-On, Y. M., Phillips, R. & Milo, R. The biomass distribution on Earth.
5. Sahu, N., Vasu, D., Sahu, A., Lal, N. & Singh, S. K. Strength of Microbes in Nutrient Cycling: A Key to Soil Health. in *Agriculturally Important Microbes for Sustainable Agriculture : Volume I: Plant-soil-microbe nexus* (eds. Meena, V. S., Mishra, P. K., Bisht, J. K. & Pattanayak, A.) 69–86 (Springer Singapore, 2017).
6. Bull, M. J. & Plummer, N. T. Part 1: The Human Gut Microbiome in Health and Disease. *Integr. Med.* **13**, 17–22 (2014).
7. Laukens, D., Brinkman, B. M., Raes, J., De Vos, M. & Vandenabeele, P. Heterogeneity of the gut microbiome in mice: guidelines for optimizing experimental design. *FEMS Microbiol. Rev.* **40**, 117–132 (2016).
8. Widder, S. *et al.* Challenges in microbial ecology: building predictive understanding of community function and dynamics. *ISME J.* **10**, 2557–2568 (2016).

9. Loutit, M. PROBLEMS IN STUDYING MICROBIAL ECOLOGY. *Proc.* **19**, 43–45 (1972).
10. Dethlefsen, L., Eckburg, P. B., Bik, E. M. & Relman, D. A. Assembly of the human intestinal microbiota. *Trends Ecol. Evol.* **21**, 517–523 (2006).
11. Gritz, E. C. & Bhandari, V. The human neonatal gut microbiome: a brief review. *Front Pediatr* **3**, 3-17 (2015).
12. Locey, K. J. & Lennon, J. T. Scaling laws predict global microbial diversity. *Proc. Natl. Acad. Sci. U. S. A.* **113**, 5970–5975 (2016).
13. Fuhrman, J. A., Cram, J. A. & Needham, D. M. Marine microbial community dynamics and their ecological interpretation. *Nat. Rev. Microbiol.* **13**, 133–146 (2015).
14. Douglas, A. E. Which experimental systems should we use for human microbiome science? *PLoS Biol.* **16**, e2005245 (2018).
15. Jessup, C. M., Forde, S. E. & Bohannan, B. Microbial experimental systems in ecology. *Adv. Ecol. Res.* **37**, 273-307 (2005).
16. Gamage, H. K. A. H. *et al.* Cereal products derived from wheat, sorghum, rice and oats alter the infant gut microbiota in vitro. *Sci. Rep.* **7**, 14312 (2017).
17. Stenuit, B. & Agathos, S. N. Deciphering microbial community robustness through synthetic ecology and molecular systems synecology. *Curr. Opin. Biotechnol.* **33**, 305–317 (2015).
18. Gresham, D. & Dunham, M. J. The enduring utility of continuous culturing in experimental evolution. *Genomics* **104**, 399–405 (2014).
19. Stein, R. R. *et al.* Ecological modeling from time-series inference: insight into

- dynamics and stability of intestinal microbiota. *PLoS Comput. Biol.* **9**, e1003388 (2013).
20. Succurro, A. & Ebenhöf, O. Review and perspective on mathematical modeling of microbial ecosystems. *Biochem. Soc. Trans.* **46**, 403–412 (2018).
21. Lenski, R. E. & Levin, B. R. Constraints on the Coevolution of Bacteria and Virulent Phage: A Model, Some Experiments, and Predictions for Natural Communities. *Am. Nat.* **125**, 585–602 (1985).
22. Lev V. Kalmykov, V. L. K. Strong violation of the competitive exclusion principle. Available from Nature Precedings <<http://hdl.handle.net/10101/npre.2011.6667.1>> (2011).
23. Thorp, J. H. Interference competition as a mechanism of coexistence between two sympatric species of the grass shrimp *Palaemonetes* (Decapoda: Palaemonidae). *J. Exp. Mar. Bio. Ecol.* **25**, 19–35 (1976).
24. Hastings, A. Spatial Heterogeneity and Ecological Models. *Ecology* **71**, 426–428 (1990).
25. Sugihara, G. *et al.* Detecting causality in complex ecosystems. *Science* **338**, 496–500 (2012).
26. Horn, H. & Lackner, S. Modeling of biofilm systems: a review. *Adv. Biochem. Eng. Biotechnol.* **146**, 53–76 (2014).
27. Toffoli, T. & Margolus, N. *Cellular Automata Machines: A New Environment for Modeling*. (MIT Press, 1987).
28. Wiedenbeck, J. & Cohan, F. M. Origins of bacterial diversity through horizontal genetic transfer and adaptation to new ecological niches. *FEMS*

- Microbiol. Rev.* **35**, 957–976 (2011).
29. Wade, M. J. *et al.* Perspectives in mathematical modelling for microbial ecology. *Ecol. Modell.* **321**, 64–74 (2016).
30. Macconkey, A. Lactose-Fermenting Bacteria in Faeces. *J. Hyg.* **5**, 333–379 (1905).
31. Novick, A. & Szilard, L. Description of the chemostat. *Science* **112**, 715–716 (1950).
32. Herbert, D., Elsworth, R. & Telling, R. C. The continuous culture of bacteria; a theoretical and experimental study. *J. Gen. Microbiol.* **14**, 601–622 (1956).
33. De Villiers, G. H. The pHauxostat. (University of Pretoria, 2001).
34. Markx, G. H., Davey, C. L. & Kell, D. B. The permittostat: a novel type of turbidostat. *Microbiology* **137**, 735–743 (1991).
35. Sikyta, B. *Techniques in Applied Microbiology*. (Elsevier, 1995).
36. Auchtung, J. M., Robinson, C. D. & Britton, R. A. Cultivation of stable, reproducible microbial communities from different fecal donors using minibioreactor arrays (MBRAs). *Microbiome* **3**, 3-42 (2015).
37. Elena, S. F. & Lenski, R. E. Microbial genetics: evolution experiments with microorganisms: the dynamics and genetic bases of adaptation. *Nat. Rev. Genet.* **4**, 457-469 (2003).
38. Liu, Z. *et al.* Ecological Stability Properties of Microbial Communities Assessed by Flow Cytometry. *mSphere* **3**, 1-13 (2018).
39. Duncan, S. H., Louis, P. & Flint, H. J. Lactate-utilizing bacteria, isolated from human feces, that produce butyrate as a major fermentation product. *Appl.*

- Environ. Microbiol.* **70**, 5810–5817 (2004).
40. Rios-Covian, D., Gueimonde, M., Duncan, S. H., Flint, H. J. & de los Reyes-Gavilan, C. G. Enhanced butyrate formation by cross-feeding between *Faecalibacterium prausnitzii* and *Bifidobacterium adolescentis*. *FEMS Microbiol. Lett.* **362**, 1-7 (2015).
 41. Marchesi, J. R. & Ravel, J. The vocabulary of microbiome research: a proposal. *Microbiome* **3**, 3-31 (2015).
 42. Guaraldi, F. & Salvatori, G. Effect of breast and formula feeding on gut microbiota shaping in newborns. *Front. Cell. Infect. Microbiol.* **2**, 94 (2012).
 43. Harmsen, H. J. *et al.* Analysis of intestinal flora development in breast-fed and formula-fed infants by using molecular identification and detection methods. *J. Pediatr. Gastroenterol. Nutr.* **30**, 61–67 (2000).
 44. Laforest-Lapointe, I. & Arrieta, M.-C. Patterns of Early-Life Gut Microbial Colonization during Human Immune Development: An Ecological Perspective. *Front. Immunol.* **8**, 788 (2017).
 45. Lau, J. T. *et al.* Capturing the diversity of the human gut microbiota through culture-enriched molecular profiling. *Genome Med.* **8**, 72 (2016).
 46. Levins, R. & Lewontin, R. C. Holism and reductionism in ecology. *Capitalism Nature Socialism* **5**, 33–40 (1994).
 47. Poeker, S. A. *et al.* Understanding the prebiotic potential of different dietary fibers using an in vitro continuous adult fermentation model (PolyFermS). *Sci. Rep.* **8**, 4318 (2018).
 48. McDonald, J. A. K. *et al.* Simulating distal gut mucosal and luminal

- communities using packed-column biofilm reactors and an in vitro chemostat model. *J. Microbiol. Methods* **108**, 36–44 (2015).
49. Paine, R. T. A Note on Trophic Complexity and Community Stability. *Am. Nat.* **103**, 91-93 (1969).
50. Fisher, C. K. & Mehta, P. Identifying keystone species in the human gut microbiome from metagenomic timeseries using sparse linear regression. *PLoS One* **9**, e102451 (2014).
51. INFORS HT - Multifors 2. Available at: <http://www.infors-ht.com/index.php/en/products/bioreactors/bench-top-bioreactors/multifors-2>. (Accessed: 27th November 2018)
52. New Brunswick Bioflo Reactors and Fermentors | Labx. Available at: <https://www.labx.com/product/new-brunswick-bioflo-reactors-and-fermentors>. (Accessed: 27th November 2018)
53. Takahashi, C. N., Miller, A. W., Ekness, F., Dunham, M. J. & Klavins, E. A low cost, customizable turbidostat for use in synthetic circuit characterization. *ACS Synth. Biol.* **4**, 32–38 (2015).
54. Matteau, D., Baby, V., Pelletier, S. & Rodrigue, S. A Small-Volume, Low-Cost, and Versatile Continuous Culture Device. *PLoS One* **10**, e0133384 (2015).
55. Toprak, E. *et al.* Building a morbidostat: an automated continuous-culture device for studying bacterial drug resistance under dynamically sustained drug inhibition. *Nat. Protoc.* **8**, 555–567 (2013).
56. Rodríguez, J. M. *et al.* The composition of the gut microbiota throughout life,

- with an emphasis on early life. *Microb. Ecol. Health Dis.* **26**, 26050 (2015).
57. *Flexostat-hardware-firmware*. (Github). Available at:
<https://github.com/Flexostat/Flexostat-interface> (Accessed: 26th November 2018)
58. *Flexostat*. (Github). Available at: <https://github.com/Flexostat> (Accessed: 26th November 2018)
59. Python, J. Python programming language. in *USENIX Annual Technical Conference* (41.203.146.53, 2007).
60. Atmel Studio 7 | Microchip Technology. Available at:
<https://www.microchip.com/mplab/avr-support/atmel-studio-7>. (Accessed: 26th November 2018)
61. Walt, S. van der, Colbert, S. C. & Varoquaux, G. The NumPy Array: A Structure for Efficient Numerical Computation. *Comput. Sci. Eng.* **13**, 22–30 (2011).
62. Liechti, C. pySerial Documentation. *Versión: 2. 6, Diciembre 2011* (2016).
63. Tatham, S., Dunn, O., Harris, B. & Nevins, J. PuTTY: A free Telnet/SSH client. Available on line at: <http://www.chiark.greenend.org.uk/~sgtatham/putty> (2006).
64. Mott, R. L. *Machine Elements in Mechanical Design* (4th. **175**, (USA: Prentice Hall, 2003).
65. Ihaka, R. & Gentleman, R. R: A Language for Data Analysis and Graphics. *J. Comput. Graph. Stat.* **5**, 299–314 (1996).
66. Wickham, H. *Ggplot2: Elegant Graphics for Data Analysis*. (Springer

- Publishing Company, Incorporated, 2009).
67. Rymovicz, A. U. M. *et al.* Screening of reducing agents for anaerobic growth of *Candida albicans* SC5314. *J. Microbiol. Methods* **84**, 461–466 (2011).
 68. Aseptic Technique. in *Current Protocols in Microbiology* (eds. Coico, R., Kowalik, T., Quarles, J., Stevenson, B. & Taylor, R.) (John Wiley & Sons, Inc., 2005).
 69. Mishra, S. & Imlay, J. A. An anaerobic bacterium, *Bacteroides thetaiotaomicron*, uses a consortium of enzymes to scavenge hydrogen peroxide. *Mol. Microbiol.* **90**, 1356–1371 (2013).
 70. Bartram, A. K., Lynch, M. D. J., Stearns, J. C., Moreno-Hagelsieb, G. & Neufeld, J. D. Generation of multimillion-sequence 16S rRNA gene libraries from complex microbial communities by assembling paired-end illumina reads. *Appl. Environ. Microbiol.* **77**, 3846–3852 (2011).
 71. Frank, J. A. *et al.* Critical evaluation of two primers commonly used for amplification of bacterial 16S rRNA genes. *Appl. Environ. Microbiol.* **74**, 2461–2470 (2008).
 72. Altschul, S. F., Gish, W., Miller, W., Myers, E. W. & Lipman, D. J. Basic local alignment search tool. *J. Mol. Biol.* **215**, 403–410 (1990).
 73. Martin, M. Cutadapt removes adapter sequences from high-throughput sequencing reads. *EMBnet.journal* **17**, 10–12 (2011).
 74. Callahan, B. J. *et al.* DADA2: High-resolution sample inference from Illumina amplicon data. *Nat. Methods* **13**, 581–583 (2016).
 75. Dixon, P. VEGAN, a package of R functions for community ecology. *J. Veg.*

- Sci.* **14**, 927–930 (2003).
76. Morris, E. K. *et al.* Choosing and using diversity indices: insights for ecological applications from the German Biodiversity Exploratories. *Ecol. Evol.* **4**, 3514–3524 (2014).
77. Ricotta, C. & Podani, J. On some properties of the Bray-Curtis dissimilarity and their ecological meaning. *Ecol. Complex.* **31**, 201–205 (2017).
78. Heck, K. L., van Belle, G. & Simberloff, D. Explicit Calculation of the Rarefaction Diversity Measurement and the Determination of Sufficient Sample Size. *Ecology* **56**, 1459–1461 (1975).
79. Roeselers, G., Zippel, B., Staal, M., van Loosdrecht, M. & Muyzer, G. On the reproducibility of microcosm experiments - different community composition in parallel phototrophic biofilm microcosms. *FEMS Microbiol. Ecol.* **58**, 169–178 (2006).
80. Antwis, R. E. *et al.* Fifty important research questions in microbial ecology. *FEMS Microbiol. Ecol.* **93**, (2017).
81. Langston, C. W., Gutierrez, J. & Bouma, C. Motile enterococci (*Streptococcus faecium* var. *mobilis* var. n.) isolated from grass silage. *J. Bacteriol.* **80**, 714–718 (1960).
82. Ziv, N., Brandt, N. J. & Gresham, D. The use of chemostats in microbial systems biology. *J. Vis. Exp.* (2013). doi:10.3791/50168
83. Frantz, J. C. & McCallum, R. E. Growth yields and fermentation balance of *Bacteroides fragilis* cultured in glucose-enriched medium. *J. Bacteriol.* **137**, 1263–1270 (1979).

84. Ramasamy, D. *et al.* Genome sequence and description of *Bacteroides timonensis* sp. nov. *Stand. Genomic Sci.* **9**, 1181–1197 (2014).
85. Lebreton, F., Willems, R. J. L. & Gilmore, M. S. Enterococcus Diversity, Origins in Nature, and Gut Colonization. in *Enterococci: From Commensals to Leading Causes of Drug Resistant Infection* (eds. Gilmore, M. S., Clewell, D. B., Ike, Y. & Shankar, N.) (Massachusetts Eye and Ear Infirmary, 2014).
86. Caflich, C., Wang, J. & Zbinden, R. The role of syringe filters in harm reduction among injection drug users. *Am. J. Public Health* **89**, 1252–1254 (1999).
87. Hygrostat/Humidistat Humidity Control. Available at:
https://www.omega.ca/pptst_eng/MFR012.html. (Accessed: 28th November 2018)
88. Ettema, C. H. & Wardle, D. A. Spatial soil ecology. *Trends Ecol. Evol.* **17**, 177–183 (2002).
89. Du, J. *et al.* Temporal and spatial diversity of bacterial communities in coastal waters of the South china sea. *PLoS One* **8**, e66968 (2013).
90. Fox, J. W. The intermediate disturbance hypothesis should be abandoned. *Trends Ecol. Evol.* **28**, 86–92 (2013).
91. Prieto-Barajas, C. M., Valencia-Cantero, E. & Santoyo, G. Microbial mat ecosystems: Structure types, functional diversity, and biotechnological application. *Electron. J. Biotechnol.* **31**, 48–56 (2018).
92. Ali Shah, F., Mahmood, Q., Maroof Shah, M., Pervez, A. & Ahmad Asad, S. Microbial ecology of anaerobic digesters: the key players of anaerobiosis.

ScientificWorldJournal **2014**, 183752 (2014).

8.0 APPENDIX I

8.1 Protocols

8.1.1 *Remotely visualizing the Pi*

The WIFI security at McMaster University, as with most academic research institutes is protected by WPA2 Enterprise technology. While this provides more security compared to other WIFI networks, it is also more restrictive to what can connect to the network. Since the Pi was not allowed to connect to the network, a protocol was created to gain access to the Pi using a personal cell phone.

Protocol

1. Turn off WIFI on phone, allowing the mobile wireless network to turn on.
2. Create a mobile wireless hotspot.
3. Wait until the Pi is recognized and shows an IP address in the mobile wireless hotspot menu.
4. Install/open the free remote access app RealVNC on cell phone.
5. Enter the Pi's credentials: user name = pi, password = raspberry, IP address from step 3.

Following the above protocol the Pi's screen was shown on a cell phone with full functionality in real time.

8.1.2 Remotely transferring data from the Pi

Protocol

1. Turn off WIFI on phone, allowing the mobile wireless network to turn on.
2. Create a mobile hotspot.
3. Connect to the mobile hotspot on the personal laptop.
4. Wait until the Pi and laptop is recognized and shows corresponding IP addresses in the mobile wireless hotspot menu.
5. Install/open Filezilla on laptop, a free File Transfer Protocol (FTP) software.
6. Enter the Pi's credentials: user name = pi, password = raspberry, IP address from step 4.
7. Copy the log files from the Pi onto the laptop.

9.0 SUPPLEMENTARY MATERIALS

Code written in Python allows users to customize the stir bar RPM and provides basic OD vs time plots. Code written in R improves data visualization and provides data analysis. These files, along with all the files needed to run the turbidostat are located on the GitHub repository <https://github.com/flettl2/turbidostat>.